2014-04-17

Metal Recovery via Automated Sortation

Hao Yu
Worcester Polytechnic Institute

Metal Recovery via Automated Sortation

by

Hao Yu

A Dissertation Submitted to the Faculty of the

WORCESTER POLYTECHNIC INSTITUTE

in partial fulfillment of the requirements for the degree of

Doctor of Philosophy

in

Material Science & Engineering

April 2014

Professor Diran Apelian, Advisor

Professor Richard D. Sisson Jr., Director of the Material Science and Engineering Program

Abstract

Each year, millions of tons of non-ferrous scrap metal are discarded in the US. This metal is wasted due to a lack of proper recovery methods. Recent developments in spectroscopic technology have made it possible to identify the waste composition of scrap metal in real-time. This has opened the door for high-speed automated metal sortation and recovery, especially for the recovery of high value precious metals, such as titanium, nickel, cobalt, molybdenum and tantalum.

Automated sortation systems typically consist of three main phases: (i) Feeding of material, (ii) Composition identification, and (iii) Physical separation. Due to their low volume and industry fragmentation, high-strength precious metal chips usually come in the form of chips smaller than 10 mm. Therefore it is extremely difficult to feed metal chips individually into the sorting system.

At CR3, a new feeding mechanism was invented and developed in order to provide single layer feeding of small metal chips. A laboratory-scale prototype was built and proven to be feasible, scalable and reliable. A model was developed to predict the output of feeding variables based on initial input parameters. An operation window of the process was also defined for various metal chip resources. These will be presented, reviewed and discussed in the following paper.

Acknowledgements

The completion of my work is connected with the support and guidance of many people.

First and foremost, I would like to extend my deepest gratitude to my advisor, Dr. Diran Apelian for his support, guidance and encouragements throughout my graduate studies. He has been an illuminated guide, not just in addressing the issues of the present work, but also in teaching me how to face the investigation and to deal with difficulties. His support is the source of my strength.

Further appreciation is due to the members of the dissertation committee, professors Richard D. Sisson Jr., Makhlouf M. Makhlouf, Libo Wang and CR3 Focus Group chair: Jeff Webster for their encouragement, critical comments and stimulating questions.

I would like to thank the members of the Center for Resource Recovery and Recycling (CR3) at the Metal Processing for their support of this work. I would like to thank Carol Garofoli, Maureen Plunkett and Rita Shilansky for making me comfortable all the time.

I would also like to thank my colleagues of MPI, Wendi Liu, Cecilia Borgonovo, Ning Sun, Eric Gratz, Lance Wu, Lei Zhang, Mei Yang and Chen Dai. Thank you for your invaluable discussion and suggestions.

Finally, but most importantly, I would like to pay my deepest gratitude and love to my family: my fiancée, Nan Bai, and my parents, Yang Yu and Suli Huang. Their love and belief in me lit my path in life and helped me strive to reach towards horizon and beyond.

Table of Content

Executive Summary

1. Introduction

Critical metals, including titanium, nickel, cobalt, and tantalum, are of great importance to us, but they are in short supply. However, compared to aluminum, copper and iron, these metals are not being recovered and recycled at a high rate. The reasons for this are complex, but perhaps the most significant reason is that there is no proper sorting technology available for this market.

The first step for metal recovery is separating metals from other waste, which is accomplished through a sorting process. Today, most metals are sorted by measuring their physical properties. For example, ferrous metals are easily separated from non-ferrous metals using magnetic separation. However, in these processes, nothing about the chemical composition of the material is known. Furthermore, in order to be successfully separated, the materials must be large enough and heavy enough to display distinct differences in physical properties.

Recent developments in sensing technologies have opened a vista of opportunities to upgrade the value of waste streams by intelligently separating out unwanted materials, leaving only the desired alloys, and identifying a specific alloy within a family of alloys. A typical automatic atomic sortation system consists of three phases: (i) Feeding onto the sensing platform, (ii) Separation, and (iii) Ejection into identified bins. Feeding is a prerequisite for the latter two phases to be carried out successfully.

In order for waste streams to be effectively scanned by the sensor and successfully separated by the ejection device, it is crucial to convey the mixed samples onto the work station individually, which is the main task of the feeding step. The focus in this process is on achieving a single-particle layer with the densest surface cover possible, but without particles touching each other.

However, unlike aluminum, copper and iron, which serve as structural components in consumer products, critical metals serve as functional components in industry products.

Therefore, the volume of critical metals in these products is small. Scraps of critical metals exist in the form of chips and fine particles, usually smaller than 10 mm in diameter.

When it comes to small particles, chips and other materials, there is no technology available for the market that can provide a mono-layer of small chips. In addition, no research addressing the issue could be found.

Therefore, the purpose of this research paper is to address a gap in the field of metal recovery and recycling: the sorting of critical metals in the form of chips. More specifically, the purpose of the research is to work on the issue of feeding small metal chips onto a sorting system for recycling and recovery. The developed technology should not only be capable of feeding chips on a laboratory scale, but should also have the potential to be commercialized.

2. Methodology

2.1 Objectives

The objective of this research is to develop an automated feeding technology to provide a monolayer of small metal chips. The chips should be in the range of 5-8 mm, or similar to the chips provided by CR3 companies, to address industrial chip attributes. The feeding technology should be able to process various chip types and have the potential to be commercialized. The technology should also offer sufficient adjustment control to fulfill different sensor and ejection parameters.

2.2 Deliverables

- A feeding technology capable of providing a mono-layer feed.
- A control algorithm to control chip feeding into the sorting system.
- An analysis to assess the potential for commercialization.

2.3 Plan of research

The research was divided into four phases. In phase one, various potential feeding technologies were investigated. The advantages and disadvantages of each method, including technical feasibility and commercial scalability, were studied and compared. The technology with the most potential, controlled rotary feeding (CRF), was selected.

In phase two, a laboratory-scale conveyor system and CRF prototype were built. A feasibility study was conducted, the results of which show that CRF is able to provide a single layer for various chip sources. Subsequently, a method was developed to analyze the chip distribution on the conveyor system. A scalability study was carried out, which showed that CRF has great potential to be commercialized. A control algorithm was developed to control chip distribution on the conveyor system.

In phase three, a model was developed to simulate the CRF process using DEM (Discrete Element Method). A model validation was conducted and the results were consistent with the experiments.

In phase four, an industrial scale CRF was constructed in cooperation with wTe. Beta trials were carried out, and the results showed that CRF is feasible at a commercial scale. The constructed model was used to predict chip distribution on a large scale, and the results were in agreement with the trial results.

3. Outcomes and conclusion

In this study, a novel feeding technology, Controlled Rotary Feeder (CRF), was designed and built. An experiment was conducted to explore the feasibility to use CRF to feed metal chips. The results show that CRF is feasible and controllable. A model was also constructed to simulate the feeding process, the results of which are in agreement with the experiments.

A commercial scale CRF was constructed at wTe. Beta trials were carried out to evaluate the feasibility and the control algorithm to control belt coverage. The results show that CRF is capable of providing a mono-layer of chips at a commercial scale. The established model was also modified to simulate beta trials and the modeled belt coverage is in agreement with experiment results.

PAPER I

Design of a New Feeding Technology for Automated Sorting of Small Metal Chips

H. Yu and D. Apelian

Center for Resource Recovery and Recycling

Metal Processing Institute

WPI, Worcester, MA 01609 USA

Keywords: Critical Metals, Scrap Recycling, Automated Sorting, Feeding

Abstract

The development in sensory technology has enabled us to recycle and recover high-value critical metals in real-time. However, being small in size, a special feeding technology is needed to allow metal chips to be sorted and separated from mixed waste. In this paper, various feeding technologies are reviewed and discussed, and a new feeding technique is developed. Laboratory-scale trials prove that the technology can provide a monolayer of small metal chips.

Introduction

Each year, millions of tons of nonferrous metals are discarded in the US [1]. These metals are wasted due to a lack of proper recovery methods. Recent developments in spectroscopic technology have made it possible to identify the composition of waste in real-time [2-7]. This has opened the door for high-speed automated metal sortation and recovery, especially for the recovery of high valued precious metals, such as titanium, nickel, cobalt, molybdenum and tantalum [8,9].

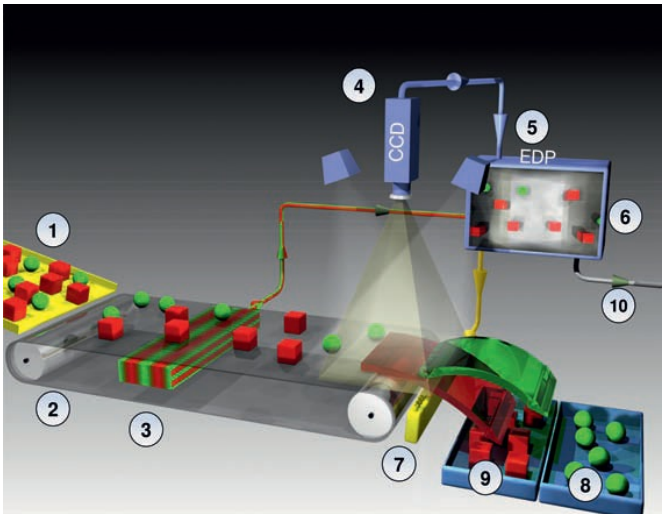

Figure 1: Schematic of automated sorting process. [10]

A schematic of an automated sorting process is shown in figure 1. A typical automatic atomic sortation system consists of three stages: (i) Feeding mixed waste onto the sorting platform, (ii) Waste composition identification, and (iii) Ejection into identified bins.

The purpose of the feeding stage is to present single particles to the sensor unit [11]. The focus in this process is on achieving a single-particle layer with the densest surface cover possible, but without particles touching each other [12]. The distance between the particles must be large enough so that a selective rejection of each single particle is possible. This is achieved by accelerating the particles and spreading them out on a larger working width than in the previous conveying mode, which leads to particles being placed further apart from each other. The first acceleration and most of the spreading of the mass stream is usually carried out by a vibrating feeder, and then the particles are conducted to the sensor system by a fast conveyor belt (in belt-type sorters) or a chute (in chute-type sorters), which the particles slide down [10].

Waste identification is the stage in which identification is carried out. Various sensing technologies could be applied, including color sensing [13-15], eddy current [16,17], and X-Ray transmission [18,19]. In this stage, every single piece of waste is scanned.

Information about the waste composition is processed through a computer and a signal is transmitted to the ejector when a foreign piece is detected.

Physical separation is the third stage. The ejection device is triggered every time any contamination is discovered by the sensor. Multiple ejection techniques can be used, but air gun ejection, mechanical ejection and water ejection are most common [20].

Sensor based sorting has advanced rapidly in the past decade. Several commercial instruments are available in the market [21,22]. It is notable that sensing and ejection technologies are very advanced: the latest sensing technology is capable of detecting particles as small as 1 mm in diameter. Meanwhile the latest ejection technology can physically separate waste with high accuracy and at ultra-high speeds.

All the three stages described contribute to the overall efficiency and accuracy of the sorting task. However, feeding is a prerequisite for the following stages. The feeding stage is essential in that successful sensing and ejection depends on the mono-layer presentation of mixed waste. Selective sorting cannot be realized without the proper feeding technique.

Figure 2: Shredded cell phone and aerospace superalloy scrap. [23]

The most notable feature for critical metals is their low volume in manufactured products. For example, the morphologies of shredded end-of-life cell phones and aerospace superalloy scrap are shown in figure 2. It can be seen that shredded end-of-life cell phones are presented in the form of very fine particles, while

aerospace waste is presented in the form of small chips. It is extremely difficult to process and sort these types of waste. This is why a special technology is needed.

Currently, when it comes to small particles, scraps, or other small materials, no proper technology is available that can provide a monolayer of small chips.

In this paper, the currently available feeding technologies are reviewed and the development of a new feeding technology is described. After conducting laboratory-scale beta trials, the results show that the new feeding technology is capable of providing a mono-layer of small metal chips.

Review of existing feeding technologies

An analysis was carried out to evaluate existing feeding technologies. Multiple industries were involved, including the metal recovery industry, plastic recovery industry, municipal waste management industry, pharmaceutical industry, food industry, and mineral processing industry.

Based on the way feeding is performed in these industries, feeding technologies can be grouped into two categories: massive feeding and individual feeding.

1. Massive feeding technology

Massive feeding technology is the most effective and reliable technique to transport and feed bulk solids. Including vibrating feeders, hopper feeders, screw feeders, apron feeders, plough feeders, and many other variations and combinations of these basic techniques, massive feeding is extensively used in the ore and mineral processing industry, waste recovery industry, municipal waste management industry, and many other such industries.

(a) Vibrating feeder:

With easy operation, low maintenance and low costs, the vibrating feeder is the dominant feeding technology used in a large number of industries.

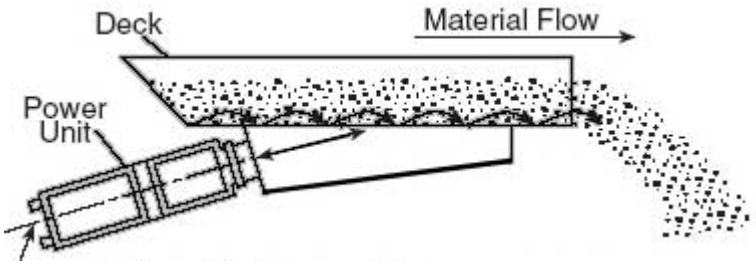

Figure 3: Vibrating feeder. [24]

A vibrating feeder consists of a feeding trough, a vibration generator, a supporting spring and a transmission device. The vibrating generator produces the vibrating motion and is normally composed of two eccentric shafts (one main, one passive) and a gear. The vibrating motion is then transferred to the feeding trough through the supporting spring. The feeding trough uses both the vibrations and gravitational force to transport and feed the bulk material to the sensor unit: the vibrations are used to move the materials, while gravity is used to control their direction.

Vibrating feeders can easily be customized to various scales because of their simple working principal and structure. Industrial vibrating feeders vary from 50 cm to 10 m in length.

Vibrating feeders are the primary technology used in the sorting industry. They are used to feed polymers, paper, large metal scraps and other waste. Vibrating feeders are highly suited to feeding large pieces of materials, but they are unsuitable for providing a monolayer of small metal chips.

(b) Screw conveyor

A screw conveyor uses a rotating helical screw blade to feed material. Normally enclosed in a tube, a screw conveyor can be used to feed or transport a wide range of materials, including food waste, wood chips, aggregates, soils, powders, or even semi-solid materials and liquids.

The working principle of a screw conveyor is illustrated in figure 4. A screw conveyor usually consists of a trough or tube containing either a spiral blade coiled around a shaft, driven at one end and held at the other, or a "shaftless spiral", driven at

one end and free at the other. The rate of volume transfer is proportional to the rotation rate of the shaft. In industrial applications the device is often used as a variable rate feeder by varying the rotation rate of the shaft to deliver a measured rate or quantity of material into a process.

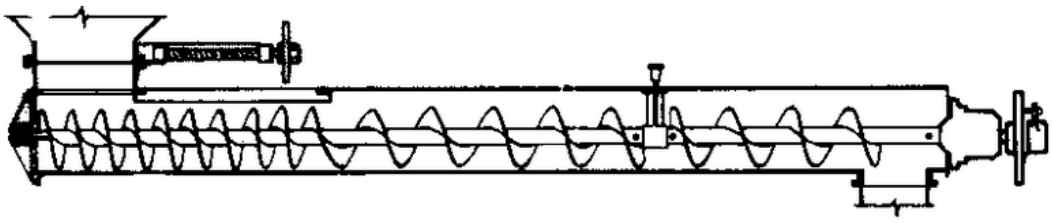

Figure 4: Screw conveyor. [25]

(c) Hopper feeder

A hopper is the one of the oldest feeding technologies. It uses gravity to feed bulk materials.

The principle is shown in figure 5. Bulk material is discharged from the top and falls along the chute onto the conveyor system. The volumetric flow rate of the feeding is controlled by the size and slope of the chute, as well as by the internal wall friction.

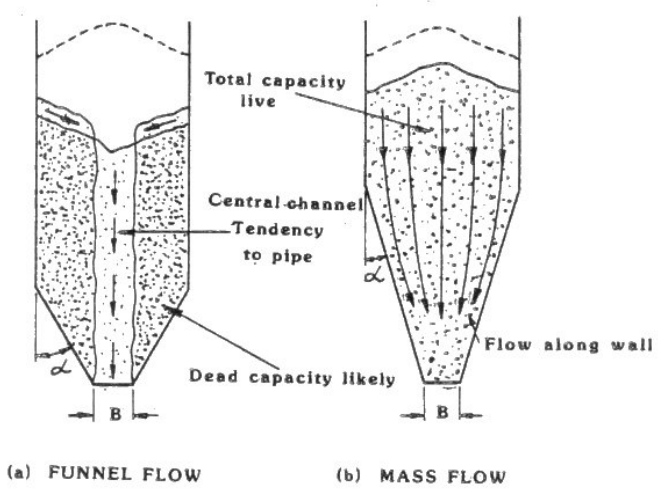

Figure 5: Material flow in a hopper feeder. [26]

2. Individual feeding technology

Individual feeding technology is used where feed needs to be isolated and presented one by one. Individual feeding is normally applied in the pharmaceutical industry, food industry, and mechanical assembly. One type of individual feeding technology is discussed below.

(a) Bowl feeder

A bowl feeder is a device used to feed small component parts individually for assembly or manufacture.

The working principle of a bowl feeder is explained in figure 6. Mixed parts are introduced into the center of the bowl feeder through a chute or a channel. The bowl feeder rotates and the mixed parts move toward the outer wall by centrifugal force. The parts are then gently shaken down to a conveyor chute which is shaped to fit their size. The parts are gradually vibrated so that they are all aligned in the same orientation. Mixed feed then exits the bowl feeder one by one, in the same orientation.

Bowl feeders are used in the consumer products industry, food industry, automotive industry, and pharmaceutical industry. Bowl feeders can be modified to suit different products by alternating the shape and size of the conveyor chute.

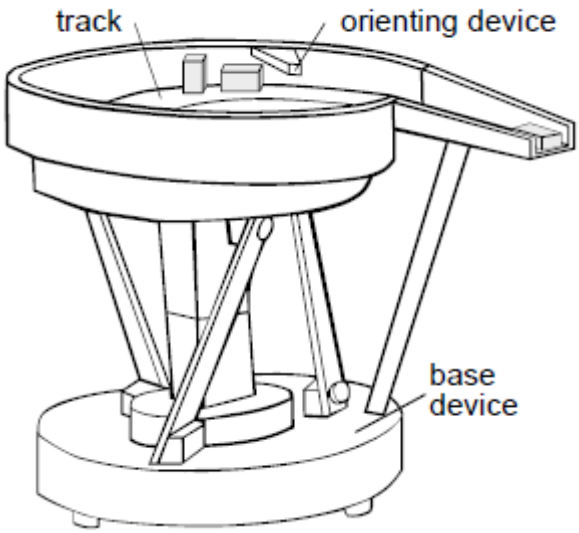

Figure 6: Bowl feeder. [27]

Materials exiting the bowl feeder are presented in a one-by-one form. Therefore, this feeding technology is capable of offering a mono-layer feed. However, the mixed material must be identical in morphology, which makes it difficult to modify this technology to handle metal chips, which are uneven in size and shape.

3. Rotary feeder

The current market provides no technology suitable to feed metal chips. Massive feeding technology is scalable, controllable and affordable. However, in massive feeding, a large number of mixed materials exit the feeding device at the same time, making it difficult to present a mono-layer material. Individual feeding technology feeds mixed materials in a one-by-one layout. This, however, means the mixed materials must be identical in size and morphology.

A feeding technology suitable for handling small metal chips must combine the features of the massive feeding and individual feeding technologies: it should have the capability to feed chips in a one-by-one pattern, while also attaining a high output rate.

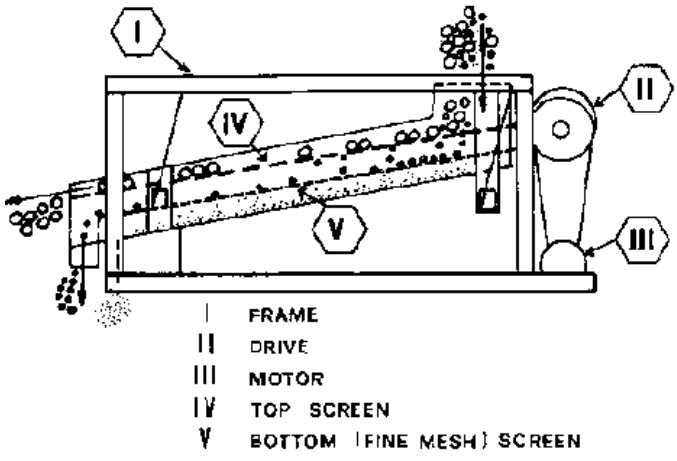

Figure 7: Schematic of rotary screener. [28]

In combining the features of the two technologies, one possibility is the usage of a rotary screener. A rotary screener, also referred to as a trommel, is a screened cylinder used to separate materials by size, as shown in figure 7. It is extensively used in the waste processing industry, for example, to separate bottles from municipal waste.

Trommels are also found in the mineral industry, where they have been used in gold mining for thousands of years. However, no effort has been made to use trommels as a feeding device.

The trommel has great potential to feed small metal chips. The screen size can be modified so that the number of chips passing through the screen holes can be controlled to achieve a monolayer. The rotating speed of the trommel can be increased to make it function as a massive feeding technology. Furthermore, the screen size can be modified according to different chip size attributes, and the trommel size can be scaled up or down easily, depending on the feeding requirement. All these features make the trommel a great candidate for this particular application.

This is why the trommel was selected as a technology to conduct research on chips feeding. In this application, the trommel designed to feed chips is referred to as the controlled rotary feeder (CRF).

Experimentation

1. Construction of a laboratory-scale rotary feeder

To evaluate the feasibility of CRF feeding, a laboratory-scale conveyor belt was designed and constructed. The laboratory-scale apparatus consisted of two parts: a conveyor belt and a control system.

The conveyor belt was a QC Industry 125 series standard conveyor, 6 inches wide and 24 inches long. The belt was a standard urethane belt driven by a dual output shaft drive pulley. The control system consisted of a Schneider Electric AC variable frequency drive and a Schneider Electric Twido series programmable logic controller. The conveyor could be programmed to operate between 0 to 150 feet per minute (FPM).

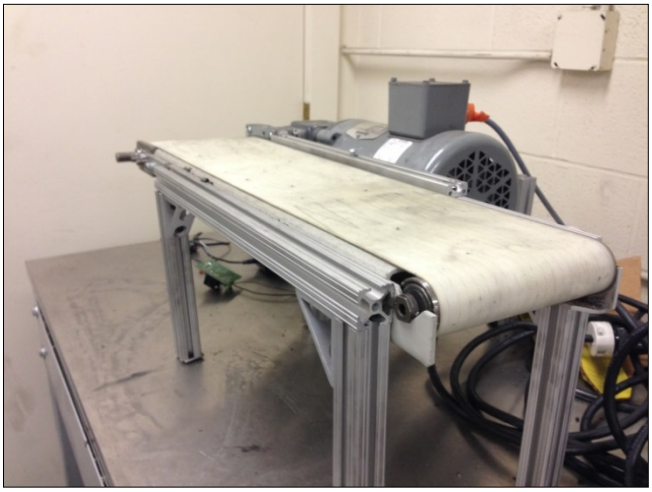

Figure 8: Lab-scale conveyor apparatus.

Subsequently, a laboratory-scale rotary feeder was designed and built, as shown in figure 9. The rotary feeder consisted of a rotary drum, an aluminum frame, a DC motor drive, and a speed controller.

The rotary drum was made of acrylic tube. The tube was ¼ inch thick and 3 inches in diameter. Holes were manually perforated. Multiple hole diameters were selected based on chip attributes. The rotary drum was secured in an aluminum frame, allowing only rotational motion. The drum was driven by a DC motor, and rotation speed was controlled by a DC speed controller.

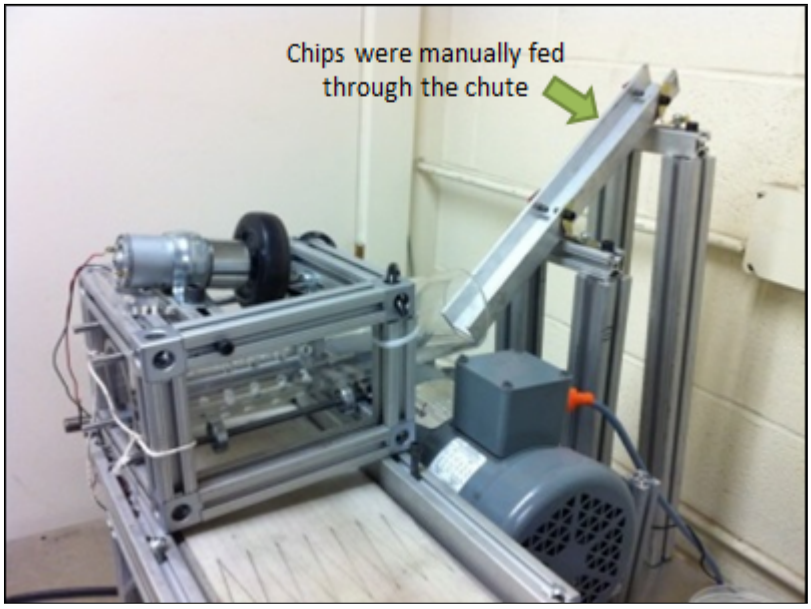

Figure 9: Laboratory-scale CRF.

2. Materials

A large number of chip materials were tested to evaluate the feasibility of CRF. The samples tested covered a wide range of metal types, including metals of different morphologies, metals that had been exposed to prior processing techniques, and metals in different contamination conditions. Some of the key metals used are summarized below.

(a) Iron machined chips

Ductile iron machined chips were provided by Victaulic. The typical chemical composition was 3.85 wt % carbon, 2.70 wt % silicon, and traces of magnesium, manganese, chromium, sulfur, phosphorus, copper, aluminium, tin, nickel, titanium, lead not exceeding a combined total of 1.0 wt %. The remainder was iron. The chips were contaminated by cutting fluid.

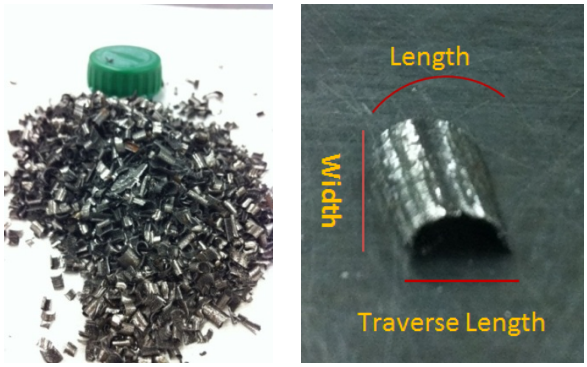

Figure 10: Morphology of iron machined chips.

The typical morphology of iron chips is curly rectangular sheets, as shown in figure 10. The curls are the result of a previous machining process. A size distribution study was conducted using a vibrating screen. The results can be seen in table I and show that iron machined chips have a small size range, with the majority in the range of 1 mm to 4.75 mm.

Table I: Iron machined chips size distribution.

Size	Combined weight (g)	Weight fraction
> 9.5 mm	2.981	1.12%
5.6 mm – 9.5 mm	2.909	1.1%
4.75 mm – 5.6 mm	2.207	0.84%
2.36 mm– 4.75 mm	124.11	46.93%
1 mm – 2.36 mm	123.88	46.84%
< 1mm	8.367	3.17%

(b) Ti-64 chips

Ti-64 chips were provided by wTe. Ti-64 is a commonly used titanium alloy. The chemical composition was 6 percent aluminum, 4 percent vanadium, 0.25 percent iron (maximum), 0.2 percent oxygen (maximum), and the remainder was titanium. The morphology of the Ti-64 chips is shown in figure 11 and typically includes tubular and arc chips. The size distribution can be seen in table II and shows that the majority of chips were in the range of 2.36 mm to 4.75 mm.

Figure 11: Morphology of Ti-64 chips.

Table II: Ti-64 chips size distribution.

Size	Combined weight (g)	Weight fraction
>5.6 mm	2.528	2.4%
>4.75 mm, <5.6 mm	3.859	3.6%
>2.36 mm, <4.75 mm	65.062	61.8%
<2.36 mm	33.836	32.1%

(c) Ti-6242 chips

Ti-6242 chips were provided by wTe. The major composition included 6 percent aluminum, 2 percent stannum, 4 percent zirconium and 2 percent molybdenum, the remainder was titanium.

The morphology of the Ti-6242 chips is shown in figure 12. The typical morphology was thin sheets. The size distribution is shown in table III. The majority of chips were in the range of 2.36 mm to 4.75 mm.

Figure 12: Morphology of Ti-6242 chips.

Table III: Ti-6242 chips size distribution.

Size	Combined weight (g)	Weight fraction
> 5.6 mm	5.503	8.68%
4.75 mm – 5.6 mm	11.732	18.50%
2.36 mm – 4.75 mm	31.899	50.3%
1 mm – 2.36 mm	11.755	18.53%
< 1mm	2.534	3.99%

3. Feasibility study

A feasibility study was carried out to evaluate the suitability of CRF for monolayer generation.

To evaluate the feeding performance, a high-speed camera system was required. A Casio EX-ZR100 camera was used. The camera was placed at three different locations to take high-speed videos: (A) at the end of the conveyor; (B) on the side of the conveyor; and (C) on top of the conveyor, as shown in figure 13. The camera recorded video at a rate of 120 frames per second, four times the speed of a regular recording. The videos were reviewed and snapshots extracted to analyze feeding performance.

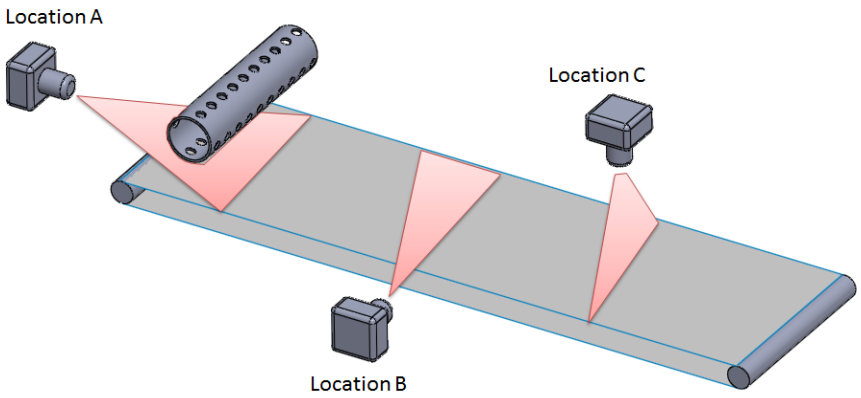

Figure 13 Camera setup for image analysis

4. Controllability study

The performance of the feeding technology was evaluated by controlling belt coverage. Belt coverage is defined as the percentage of belt surface that is covered by a mono-layer of chips.

Various levels of belt coverage must be obtained to meet the requirements of sensing and ejection technologies. As the belt was moving at a high speed, videos of the chips moving on the conveyor belt were recorded with the camera placed at location C. Subsequently, images were extracted from the videos and converted into a binary image. Belt coverage was obtained by using Matlab and calculating the black area of the binary image.

A comparison of an image extracted from the feeding video and the converted binary image is illustrated in figure 14.

Figure 14: Comparison of image extracted from feeding video (left) and the converted binary image (right).

Results and Discussion

1. Feasibility

A feasibility study was carried out to evaluate CRF's capability of monolayer generation. The high-speed camera system was placed at locations A and B to record videos of the moving conveyor belt, as described in figure 13. To evaluate feeding performance, videos were visually inspected and snapshots were extracted every 0.05 seconds.

Snapshots of feeding iron chips are shown in figures 15 and figure 16. In figure 15, one can observe the chips passing through the rotary feeder and falling onto the conveyor belt individually. The screen size for feeding iron chips was 8 mm, which allowed for individual feeding: only one chip passed the screen hole at a time. When

the chips fell on to the surface of the conveyor belt, they bounced less than two times and a monolayer of chips was achieved. Snapshots from location B further confirm the realization of a monolayer (figure 16).

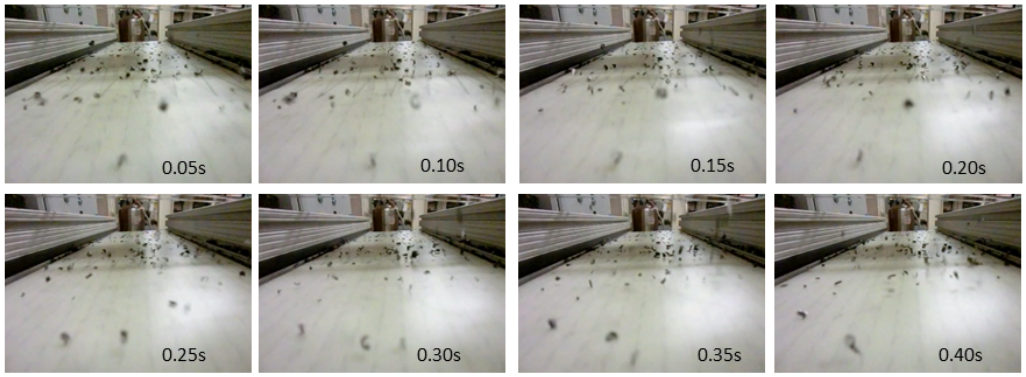

Figure15: Slow motion of iron chips feeding from location A.

Figure 16: Slow motion of iron chips feeding from location B.

Similar results could be found for Ti-64 chips and Ti-6242 chips, as shown in figure 17 and figure 18.

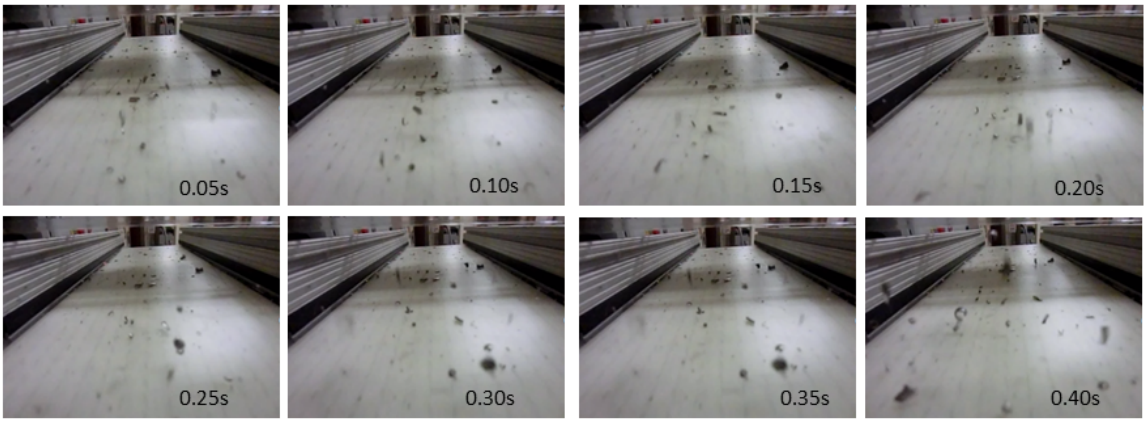

Figure 17: Slow motion of Ti-6242 chips feeding.

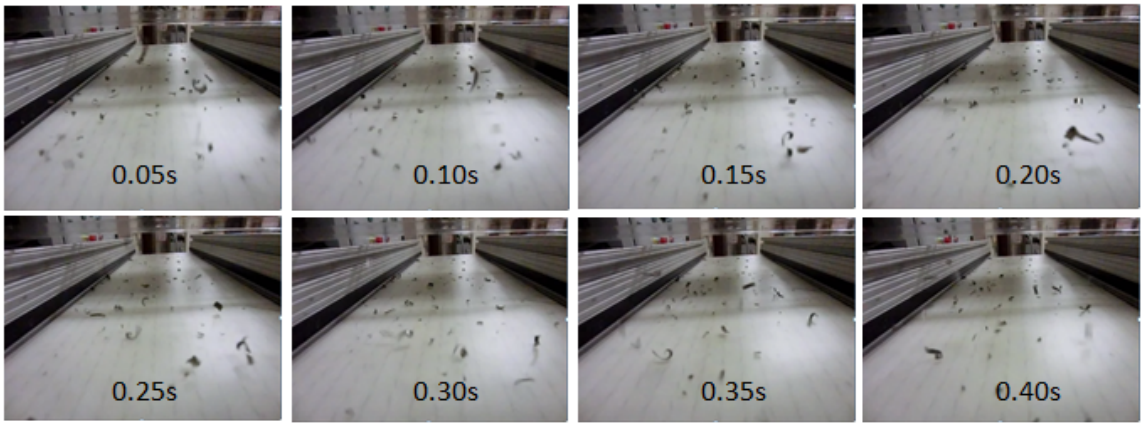

Figure 18: Slow motion of Ti-64 chips feeding.

2. Controllability study

For successful selective sorting, the control of belt coverage must meet the requirements of various sensing and ejection technologies.

In the operation of CRF, three variables have major influence on belt coverage: feed rate, drum speed, and belt speed. To explore the control algorithm of CRF, experiments were conducted to study belt coverage under different operational conditions.

In these experiments, a high-speed camera system was placed at location C, as illustrated in figure 13. Twenty snapshots were extracted from the feeding videos. Belt coverage was calculated and averaged for the extracted images. Iron machined chips were selected to conduct the study.

(a) Alternating feed rates

Experiments were conducted to study how belt coverage changes when the feed rate is altered. The belt speed was maintained at 100 FPM, and the drum speed was maintained at 60 rounds per minute (RPM). Five feed rates were tested: 10 kg/hr, 20 kg/hr, 30 kg/hr, 40 kg/hr, and 50 kg/hr. Belt coverage data for each feed rate was averaged from six repeated experiments.

The relationship between feed rate and belt coverage is shown in figure 19. It can be seen that belt coverage is linear with feed rate. Examples of extracted snapshots are shown in figure 20. One can see that as feed rate increases, more chips fall onto the conveyor belt at the same time. The distance between chips reduces, meaning a higher belt coverage is obtained.

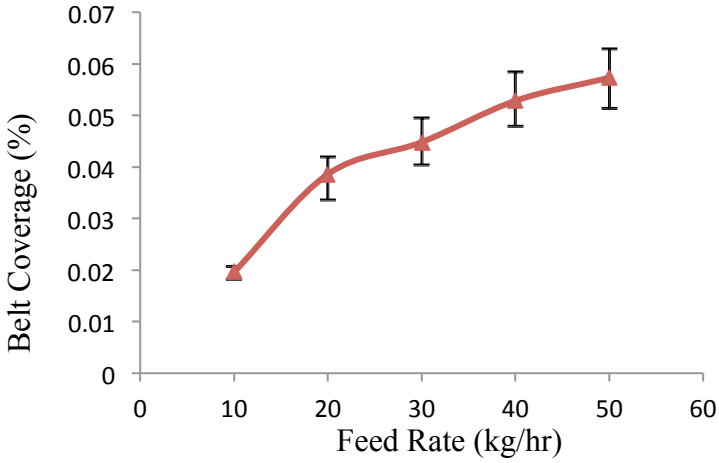

Figure 19: Belt coverage versus feed rate.

(Iron chips, belt speed: 100 FPM, drum speed: 60 RPM)

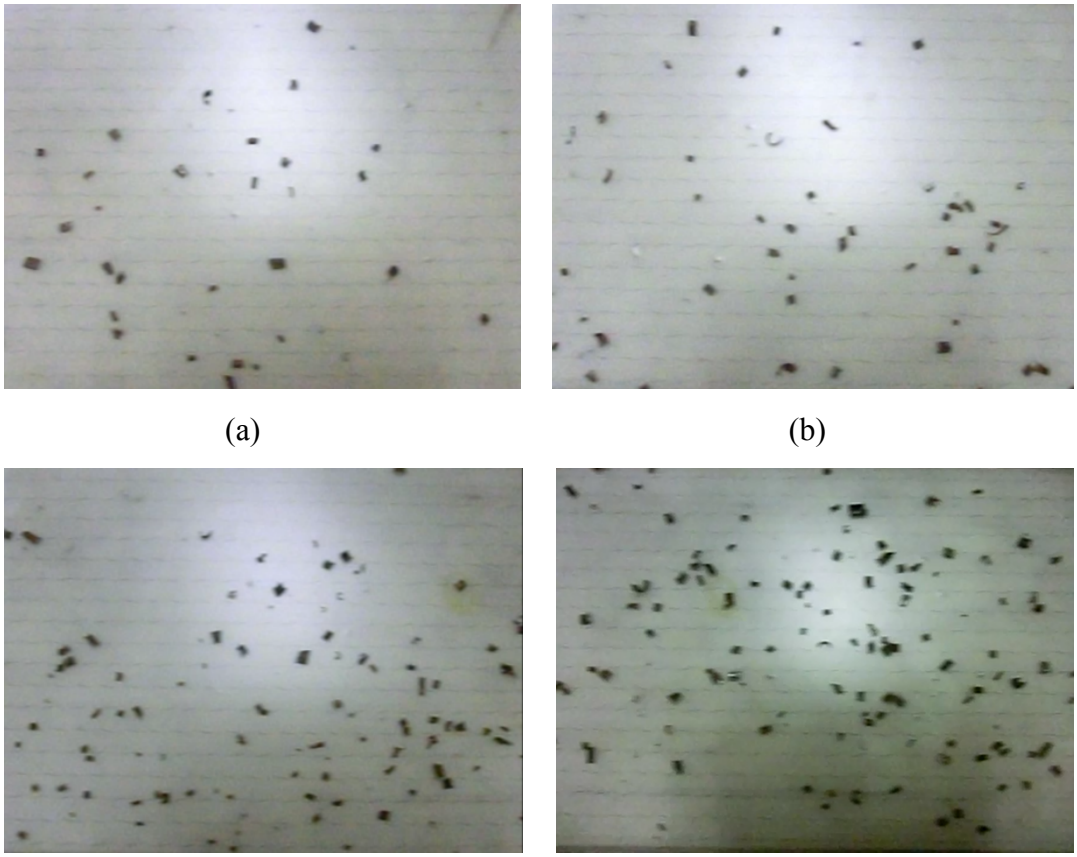

(a) (b)

(c) (d)

(e)

Figure 20: Snapshots of iron chips feeding at various feed rates

(a) 10 kg/hr, (b) 20 kg/hr, (c) 30 kg/hr, (d) 40 kg/hr, (e) 50 kg/hr

(b) Alternating belt speeds

For this experiment, the feed rate was fixed at 30 kg/hr, and the drum speed was set at 60 RPM. Six belt speeds were tested: 100 FPM, 110 FPM, 120 FPM, 130 FPM, 140 FPM and 150 FPM. The results are shown in figure 21. It can be seen that belt coverage decreases as belt speed increases. The feeding images at various belt speeds demonstrate this trend clearly, as shown in figure 22.

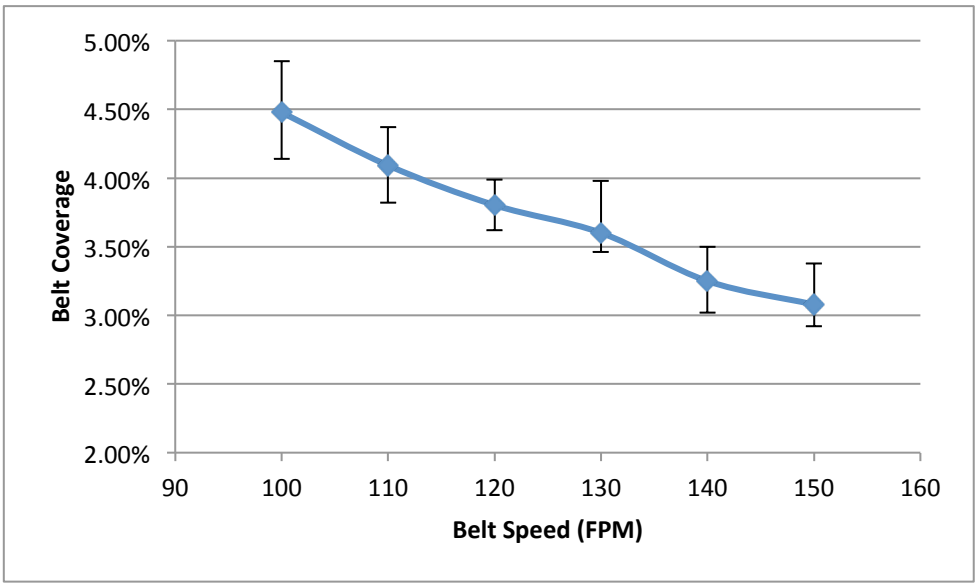

Figure 21: Belt coverage vs belt speed.
(Iron chips, feed rate: 30 kg/hr, drum speed: 60 RPM)

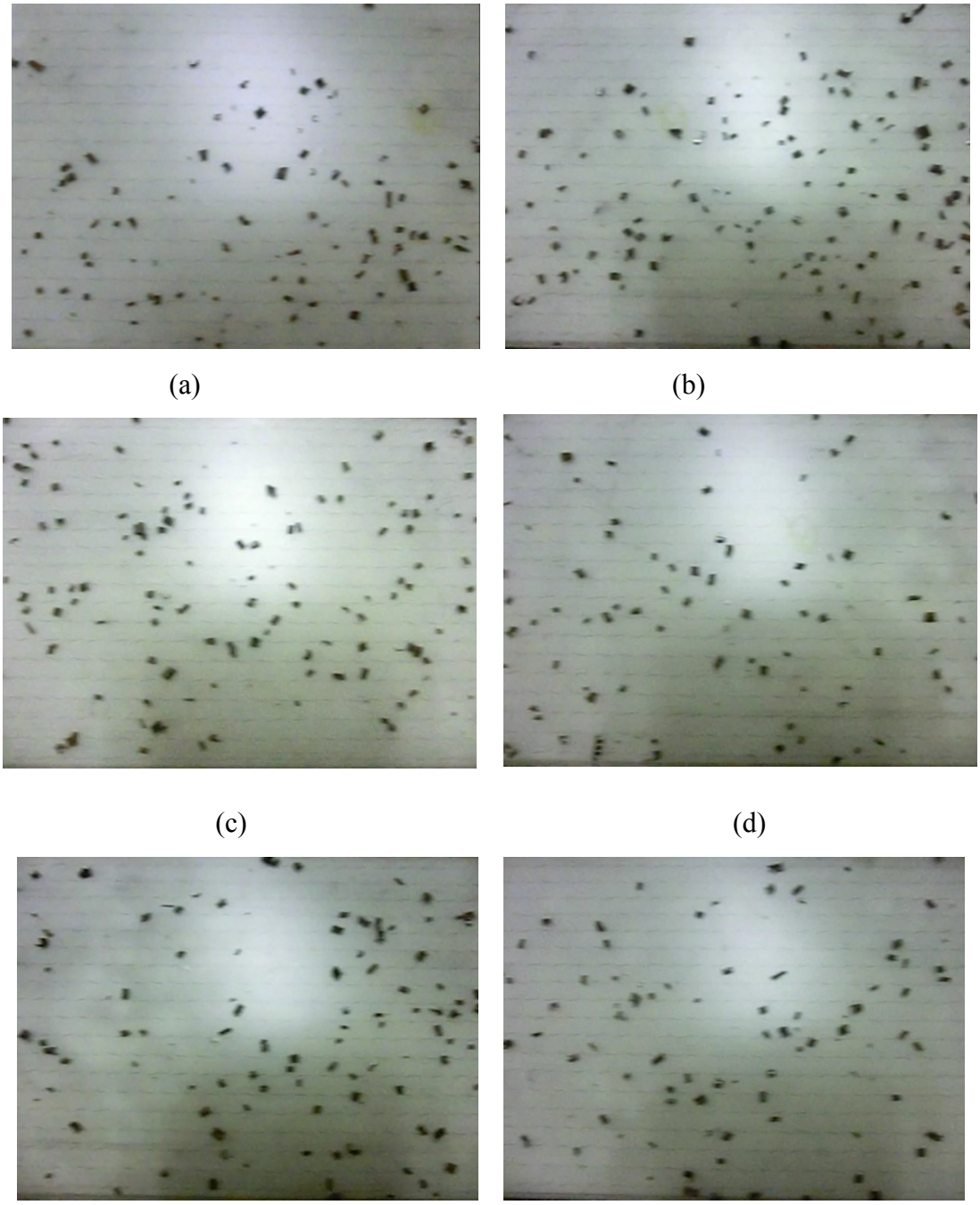

(a) (b)

(c) (d)

(e) (f)

Figure 22: Snapshots of iron chips feeding at various belt speeds

(a) 100 FPM, (b) 110 FPM, (c) 120 FPM (d) 130 FPM, (e) 140 FPM, (f) 150 FPM

Conclusion

Automated sorting systems provide a powerful tool to recover and recycle high-value critical metals. However, due to low volumes and low industrial fragmentation, a special feeding technology is needed to handle small metal chips (less than 5 mm in diameter). Currently, no technology suitable for feeding metal chips is available in the market.

In this paper, the development and performance of a new feeding technology, controlled rotary feeder (CRF), is described. An analysis is conducted to explore the feasibility of using CRF to feed metal chips. The results show that CRF is a feasible technology to feed small metal chips. Various belt coveragess can be attained to meet the requirements of various sensing and ejection technologies.

References

[1] D. B. Spencer, "The High-Speed Identifi cation and Sorting of Nonferrous Scrap," JOM, pp. 46 - 51, Apr 2005.

[2] S. Koyanaka and K. Kobayashi, "Automatic sorting of lightweight metal scrap by sensing apparent density and three-dimensional shape," Resources, Conservation and Recycling, vol. 54, p. 571–578, 2010.

[3] M. Mesina, T. d. Jong and W. Dalmijn, "Automatic sorting of scrap metals with a combined electromagnetic and dual energy X-ray transmission sensor," Int. J. Miner. Process, vol. 82, pp. 222-232, 2007.

[4] S. Zhang, E. Forssberg, B. Arvidson and W. Moss, "Aluminum recovery from electronic scrap by High-Force® eddy-current separators," Resources, Conservation and Recycling, vol. 23, pp. 225-241, 1998.

[5] R. Noll, H. Bette, A. Brysch, M. Kraushaar, I. Monch, L. Peter and V. Sturm, "Laser-induced breakdown spectrometry — applications for production control and quality assurance in the steel industry," Spectrochimica Acta Part B, vol. 56, pp. 637-649, 2001.

[6] R. Noll, V. Sturm, Ü. Aydin, D. Eilers, C. Gehlen, M. Höhne, A. Lamott, J.

Makowe and J. Vrenegor, "Laser-induced breakdown spectroscopy:From research to industry, new frontiers for process control," Spectrochimica Acta Part B, vol. 63, pp. 1159-1166, 2008.

[7] T. Pretz and D. Killmann, "Possibilities of sensor based sorting regarding recycling of waste," Acta Metallurgica Slovaca, Vols. 188-193, p. 12, 2006.

[8] R.L.Moss, E.Tzimas, H.Kara, P.Willis and J.Kooroshy, "Critical Metals in Strategic Energy Technologies," European Commission Joint Research Centre, 2011.

[9] M. Buchert, A. Manhart, D. Bleher and D. Pingel, "Recycling critical raw materials from waste electronic equipment," 2012.

[10] H. Wotruba and H. Harbeck, "Sensor-Based Sorting," Ullmann's Encyclopedia of Industrial Chemistry., vol. 32, pp. 395-404, 2010.

[11] H.R.Manouchehri, "Sorting: Possibilities, Limitations and Future".

[12] H. Wotruba, "State-of-the-art of Sensor-Based Sorting," BHM , vol. 6, pp. 221-224, 2008.

[13] R. Wyss and Schultz.P.B, "Color Sorting Aluminum Alloy for Recycling," The Minerals, Metals & Materials Society, pp. 1093-1098, 1999.

[14] J. Kolacz and J. Chmelar, "Cost Effective Optical Sorting System," Recycling and Waste Treatment in Mineral and Metal Processing: Technical and Economic Aspects, pp. 313-322, 2002.

[15] W. Forsthoff, "Optical Sorting of Coarse Materials," ZKG International , vol. 53, pp. 329-331, 2000.

[16] S. E, "Eddy current techniques for segregating nonferrous metals from waste," Conserv, vol. 5, pp. 149-162, 1982.

[17] F. E. Zhang S, "Eddy current separation technology: overview, fundamentals and

applications," MIMER Report No. 7.Lulea˚, Sweden: Division of Mineral Processing, Lulea˚ University of Technology, 1997.

[18] T.D.W.de Jong, "X-ray transmission imaging for process optimisation of solid resources," Proceedings R'02 Congress,, 12-15 Feb 2002.

[19] W. D. a. H. K. T.P.R. de Jong, "Dual energy X-ray transmission imaging for concentration and control of solids," XXII International Mineral Processing Congres - IMPC, Cape Town, 2003.

[20] U. Habich, "Sensor-Based Sorting Systems in Waste Processing".

[21] WRAP MDD018/23 WEEE Separation Techniques Titech NIR sorting trial report.

[22] "A Review of Optical Technology to Sort Plastics & Other Containers," Environment & Plastics Industry Council, 2008.

[23] J. Neira, "End-of-Life Management of Cell Phones in the United States," 2006.

[24] "HP Electromagnetic Vibrating Feeders," Jeffrey Rader, [Online]. Available: http://www.jeffreyrader.com/feeders/HP_Electromagnetic_Feeders.cfm.

[25] A. Roberts, "Design and Application of Feeders for the Controlled Loading of Bulk Solids onto Conveyor Belts," Department of Mechanical Engineering The University of Newcastle N.S.W., Australia..

[26] W. Y. and S. L. Dickerson, "Modeling and Control of A Novel Vibratory Feeder," Proceeding of the 1999 IEEE/ASME International Conference on Advanced Intelligent Mechatronics, 1999.

[27] P. Wolfsteiner and F. Pfeiffer, "Modeling, Simulation, and Verification of the Transportation Process in Vibratory Feeders," vol. 80, pp. 35-48, 2000.

[28] "Feed screeners, sieves and seperators," http://www.feedmachinery.com/, [Online]. Available: http://www.feedmachinery.com/glossary/equipment/sieve/.

PAPER II

Design of a New Feeding Technology for Feeding Small Metal Chips – Controlling and Modeling

H. Yu and D. Apelian

Center for Resource Recovery and Recycling

Metal Processing Institute

WPI, Worcester, MA 01609 USA

Keywords: Critical Metals, Scrap Recycling, Feeding, DEM Simulation

Abstract

Resource recovery and recycling is becoming more and more critical for a sustainable future, especially recovery of high-value, critical metals. But due to low volume and low industry fragmentation, critical metals are not being recycled at a high rate. The recovery of critical metals requires metal scraps to be fed in a monolayer form, however, no such technology is available for this market. At the Center for Resource Recovery and Recycling (CR3), a controlled rotary feeder (CRF) was developed and proven to be a feasible solution for feeding a monolayer of metal scrap particles. In this paper, the controlling of CRF is discussed. A model was established to simulate a feeding process using the discrete element method (DEM). Laboratory-scale trials were conducted to validate the model and the results show that the model can predict the feeding parameters with high accuracy.

Introduction

Each year, millions of tons of nonferrous metals are discarded in the US [1]. These metals are not reused due to a lack of effective recovery methods. Recent developments in spectroscopic technology have made it possible to identify the composition of waste in real-time [2-7]. This has opened the door for high-speed automated metal sortation and recovery, especially for the recovery of high-value precious metals, such as titanium, nickel, cobalt, molybdenum and tantalum [8] [9].

Sensor-based sorting technology has developed rapidly over the past decade. Several commercial technologies are available in the market, such as X-Ray transmission [10,11], eddy current separation [12,13], and color separation [14-16]. These techniques are extensively used in the sortation of steel, iron, aluminum and other such materials. However, when it comes to high–value, critical metals, recovery methods have not yet been optimized.

A typical automatic sortation system consists of three stages [17]: (i) Feeding mixed waste onto the sensing platform, (ii) Waste composition identification, and (iii) Ejection into identified bins. It is important to note here that existing sensing and ejection technologies are very advanced: the latest sensing technology is capable of detecting particles as small as 1 mm in diameter, and ejection technology can physically separate waste with high accuracy and at ultra-high speeds.

These three stages contribute to the overall efficiency and accuracy of the sorting task. However, feeding is a prerequisite for the following stages. The feeding stage is essential in that the sensing and ejection stages depend on the mixed waste being presented in a monolayer. Therefore, successful selective sorting cannot be achieved without a proper feeding technique. Currently, the situation is that when it comes to small particles, scraps, or other small materials, no proper technology is available that can provide a monolayer of small chips.

At the Center for Resource Recovery and Recycling (CR3), a controlled rotary feeder

(CRF) was developed. A laboratory-scale prototype was designed and built, and a feasibility study shows that it is a feasible technology to feed metal scraps in a monolayer.

The success of intelligent sorting relies on scrap particles being fed in a monolayer at a controlled distance from each other. Controlling is essential for intelligent sorting in that the chips should be distributed uniformly so that no chips are touching one another. In addition, the distance between chips should be controlled in order to remove any contaminants while minimizing the number of clean material removed to maximize yield. As the conveyor belt is in motion, it is challenging to measure the distance between chips. Defined as a percentage of belt area covered by monolayer scrap particles, belt coverage is normally used to analyze chip distance.

In this paper, various feeding parameters are discussed and an algorithm to control belt coverage is developed. A model is also established to simulate the feeding process and predict belt coverage. The results show that the model is able to predict belt coverage with high accuracy.

CRF feeding process

The working principal of CRF feeding is illustrated in Figure 1.

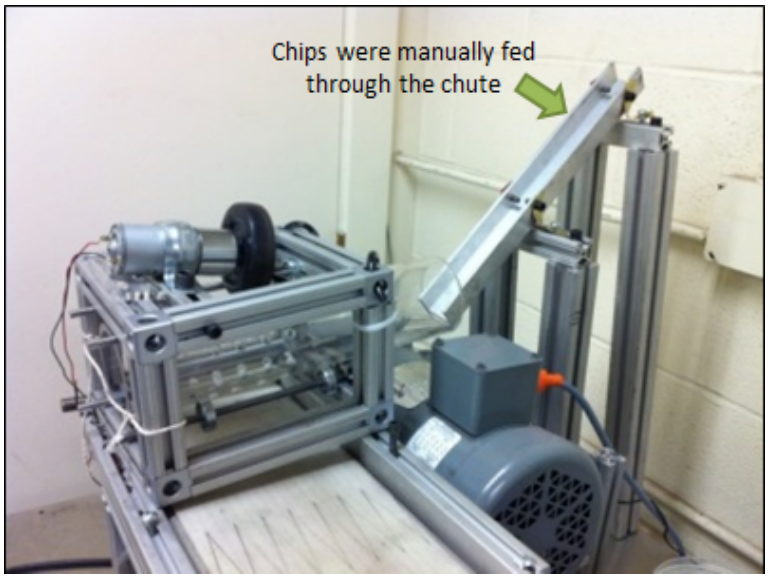

Figure 1: Principal of CRF feeding.

The CRF consists of a perforated rotary drum, an aluminum frame, a DC motor drive and a speed controller. The CRF works similarly to a trommel, which is used to separate materials by size. Scrap particles are fed into the drum through the chute, as illustrated in figure 1. Once chips are fed into the drum, the drum rotates and chips move along the drum as the result of rotation. As chips move inside the drum, some chips pass through the holes of the surface of the drum and fall onto the surface of the conveyor belt. Chips that do not pass through the holes eventually exit the drum and are collected at the end of the drum. These chips are normally oversized chips.

CRF feeding is a complex process with many parameters involved. The variables can be grouped into two categories: fixed variables and adjustable variables.

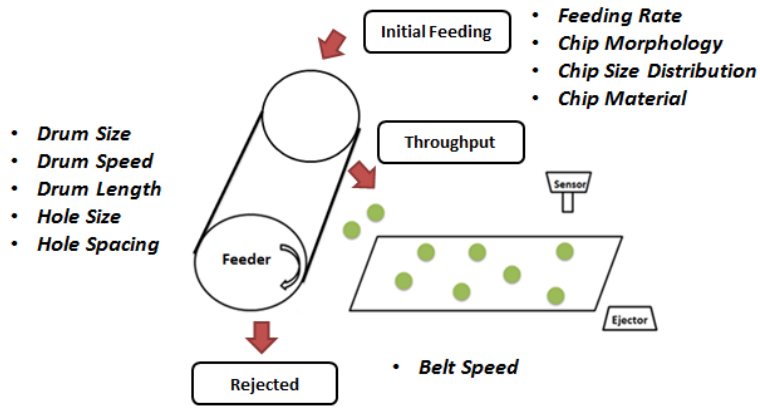

Figure 2: Variables involved in CRF feeding.

(a) Fixed variables

Fixed variables are variables that are determined prior to the operation of CRF, including chip attributes, hole size, hole distribution, drum length and drum diameter. These variables cannot be altered during CRF operation.

Chip attributes include chip material, chip morphology, and chip size distribution. These attributes are predetermined by the type of chips that are being sorted. Chip attributes also determine other operational parameters, including hole size and hole distribution.

The hole size is determined by the size of the chips. The maximum size of particles that should pass through the screen determines the minimum hole size.

However, chips ranging from half the nominal hole size (half-size) to the nominal size show much lower screening efficiencies than smaller particles. Therefore, the size of hole should be at least twice the largest chip size [18].

The drum length and drum diameter are determined by the size of the conveyor. The drum length is determined by the dimensions of the conveyor belt systems. Normally, the length of the drum should be identical to the width of the conveyor belt.

(b) Adjustable variables

Adjustable variables are variables that can be altered in the operation of CRF to control feeding performance. Variable parameters include feed rate, drum speed and belt speed.

The feed rate is the volumetric flow of the chip input. It is one of the major operation variables that can be altered and is determined by the size of the drum and the designed production rate. A higher feed rate is always desirable, however, the feed rate has a major influence on belt coverage. Normally, the higher the feed rate, the higher the belt coverage.

The drum speed is an important variable in the operation of CRF. It primarily affects the behavior of the material inside the drum. The drum speed is usually determined relative to the so-called critical speed, which is the angular velocity that produces a centripetal acceleration of 1 g at the screen surface. The formula for critical speed (Rc) is given by:

$$R_c = (2\,\mathrm{g}/\,\mathrm{D})^{0.5} / 2\pi$$

where g is the gravitational acceleration and D the diameter of the drum.

At critical speed, material normally remains stuck to the drum surface and the drum plugs. At about 75 percent of critical speed, violent agitation tends to keep the material in the air and away from the holes. At very low speeds, tumbling action is poor, limiting efficiency, and the drop height is low, limiting total

throughput. Normally, drum speed is specified as 30 – 50 percent of the critical speed.

Belt speed is determined mainly by the limitations of the sensor and the ejector, as well as by the attributes of the materials being sorted and the desired production rate. To increase production rate, belt speed should be as high as possible. However, a high belt speed means there is insufficient time for sensing and ejecting, which decreases the accuracy of the sorting.

Model

Since many variables are involved in CRF feeding, a model was developed to simulate the process. The discrete element method was used. Unlike the traditional finite element method, which considers the object as a continuous body and solves the problem by calculating partial differential equations, discrete element modeling considers the bulk solid as a system of interacting bodies. Each particle in the system is treated separately, having its own mass, velocity and contact properties [19].

1.1 Model construction

In DEM modeling, interactions between every single chip and between chips and the environment (i.e. rotary feeder and conveyor belt) are calculated and numerically integrated. Therefore, the model allows the simulation of the entire feeding process, from chips being fed into the rotary feeder to chips being transported on the conveyor belt. Moreover, various parameters can be addressed and simulated, including chip morphology, chip property, chip size distribution, initial feed rate, drum diameter, drum length, drum rotation speed, screen size and belt speed.

1.1.1 Chip morphology

The generation of elemental particles to represent iron chips is shown in figure 3 as an example.

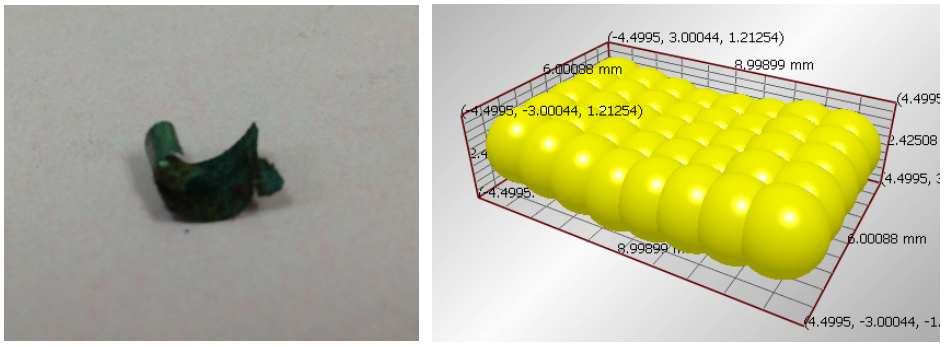

Figure 3: EDEM elemental particle configuration to represent chip morphology.

Instead of assuming that all particles are shaped as a sphere, non-spherical particles were created to characterize various particle morphologies. This process was accomplished by generating complex multi-element particles from simple spherical elements, and merging these elements as a single particle. Properties of the created multi-sphere particle, including moments of inertia and mass, were calculated for the simulation.

1.1.2 Feeder geometry

The geometry of the rotary feeder and conveyor belt system was generated using Solidworks. Subsequently, the geometry was imported into EDEM, a commercially available simulation software. The imported geometry is shown in figure 4. The size of the feeder and the drum represent the actual proportions of the laboratory equipment used.

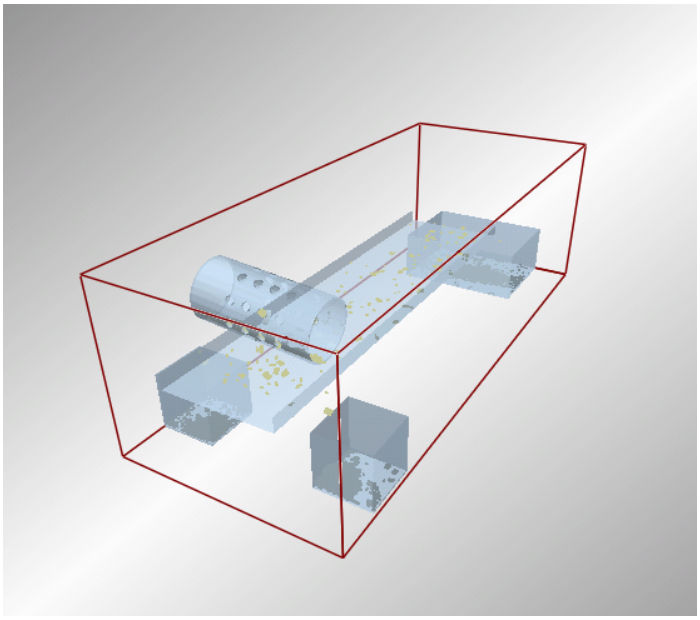

Figure 4: Imported feeder geometry.

1.1.3 Contact force

Hertz-Mindlin contact force was used to calculate interactions. In Hertz-Mindlin contact mode, the particles are allowed to overlap and the amount of overlap (Δx), and normal and tangential relative velocities determine the collisional forces via Hertz-Mindlin law [20].

The normal force (F_n) is a function of normal overlap (δ) and is given by:

$$F_n = \frac{4}{3} E^* \sqrt{R^*} \delta_n^{\frac{3}{2}}$$

where the equivalent Young's Modulus (E^*) and the equivalent radius (R^*) are defined as

$$\frac{1}{E^*} = \frac{(1-\nu_i^2)}{E_i} + \frac{(1-\nu_j^2)}{E_j}$$

$$\frac{1}{R^*} = \frac{1}{R_i} + \frac{1}{R_j}$$

with E_i, v_i, R_i and E_j, v_j, R_j, being the Young's Modulus, Poisson ratio and radius of each sphere in contact.

The tangential force (F_t) depends on the tangential overlap (δ_t) and the tangential stiffness (S_t).

$$F_t = -S_t \delta_t$$

where

$$S_t = 8G^* \sqrt{R^* \delta_n}$$

Here G* is the equivalent Shear Modulus.

1.1.4 Material properties

Material properties, including density, Shear Modulus and Poisson's ratio, were used to calculate contact forces. The interactions between chips, between chips and the drum, and between chips and the conveyor belt, were determined by the properties of each of the three components.

Values of density, Shear Modulus and Poisson's ratio were referred and assigned to the chips, rotary feeder and conveyor belt respectively, as shown in table I.

Table I: Material properties imported for the model.

	Chip density (kg/m^3)	Shear Modulus (Pa)	Poisson's ratio
Iron chips	7800	$8e^{+10}$	0.32
Ti-6242 chips	4650	$4e^{+10}$	0.33
Ti-64 chips	4430	$4e^{+10}$	0.342
Rotary drum	1200	$3e^{+9}$	0.4
Conveyor belt	1100	$1e^{+7}$	0.45

1.1.5 Feeding parameters

As the sizes of chips are not identical, chip size distribution data was obtained using a vibrating screen and imported into EDEM. Feed rate, belt speed and drum speed were also imported.

1.2 Model output

The simulated feeding process is shown in figure 5. Figure 5(a) is the entire feeder-conveyor system at 0 seconds. No chip is observed in the system. The drum starts rotating and the first chip enters the drum at 0.03 seconds, as shown in figure 5(b). More chips are fed into the drum and chips are accumulated in the drum as the process continues (figure 5(c)). At 1 second, chips start to pass through the hole of the drum and fall onto the conveyor belt, as shown in figure 5(d). As the feeding process continues, chips are continuously fed through the rotary feeder, as shown in figure 5 (e), (f) and (g).

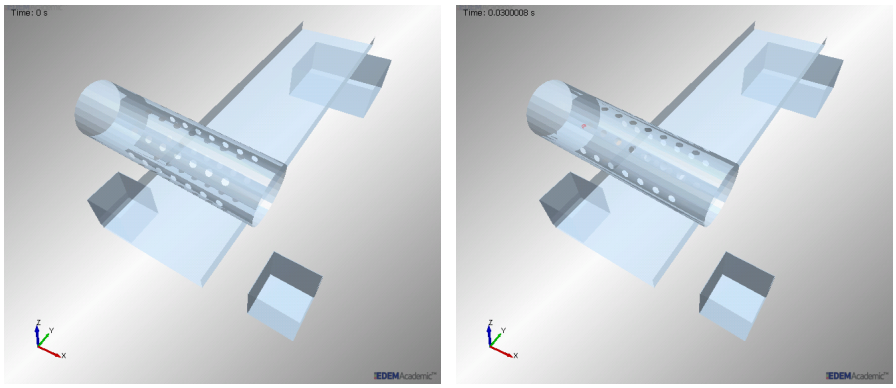

(a) (b)

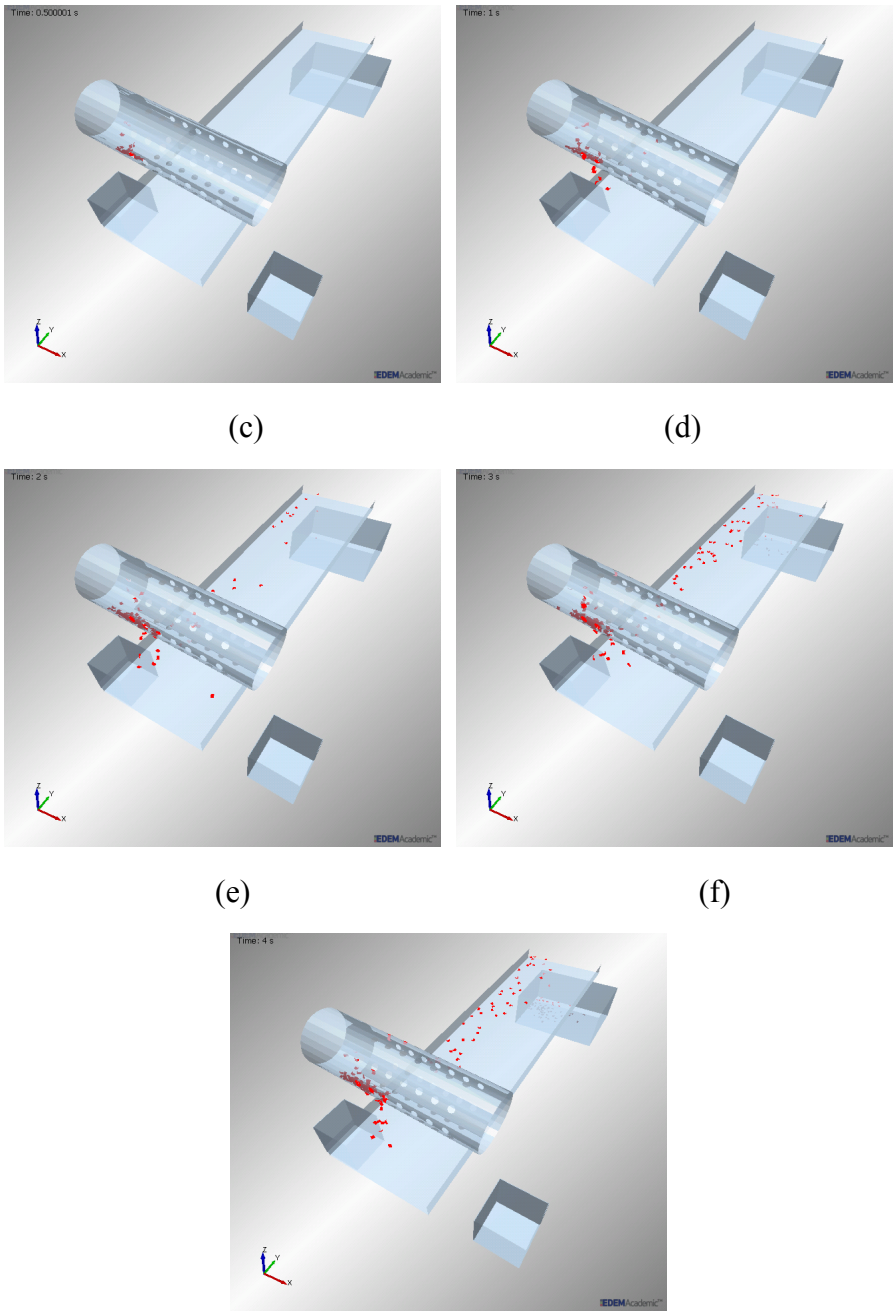

(c) (d)

(e) (f)

(g)

Figure 5: Modeled rotary feeding process.
(a) zero seconds; (b) 0.03 seconds, (c) 0.5 seconds, (d) 1 second,
(e) 2 seconds, (f) 3 seconds, (g) 4 seconds

1.3 Model validation

Experiments were conducted to validate the model.

As the conveyor is moving at ultra-high speed, it is impossible to examine belt

coverage manually. Therefore a camera-aided image analysis algorithm was developed.

Videos of chips moving on the conveyor belt were recorded by a high-speed camera, which was placed above the conveyor, as illustrated by location C in figure 6. Videos were visually inspected and snapshots were extracted to analyze feeding performance. Subsequently, the snapshots were converted into binary images. An image of belt coverage was obtained in Matlab by calculating the portion of black area in the binary image. Similarly, belt coverage from simulations was also calculated using Matlab.

A comparison of an image extracted from the feeding video and a converted binary image is illustrated in figure 7.

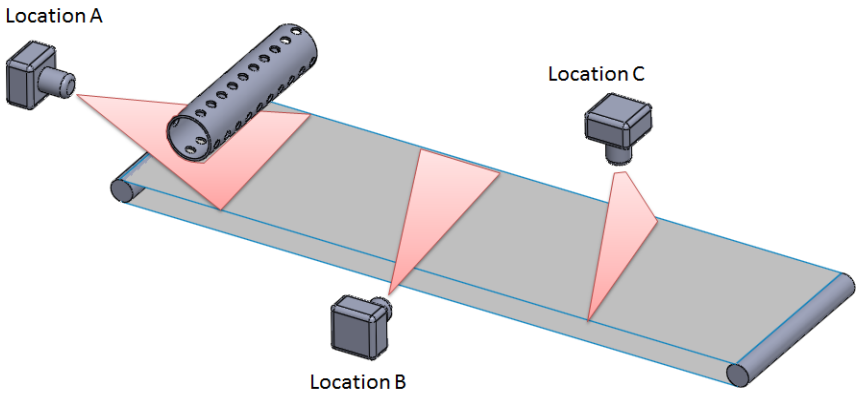

Figure 6: Camera setup for image analysis.

Figure 7: Comparison of image extracted from feeding video (left) and the converted binary image (right).

Comparisons between the images of the experiment and the simulation are shown in figure 8. Snapshots were extracted every one second. Through a visual inspection, it is possible to see that the images and simulations are in good agreement.

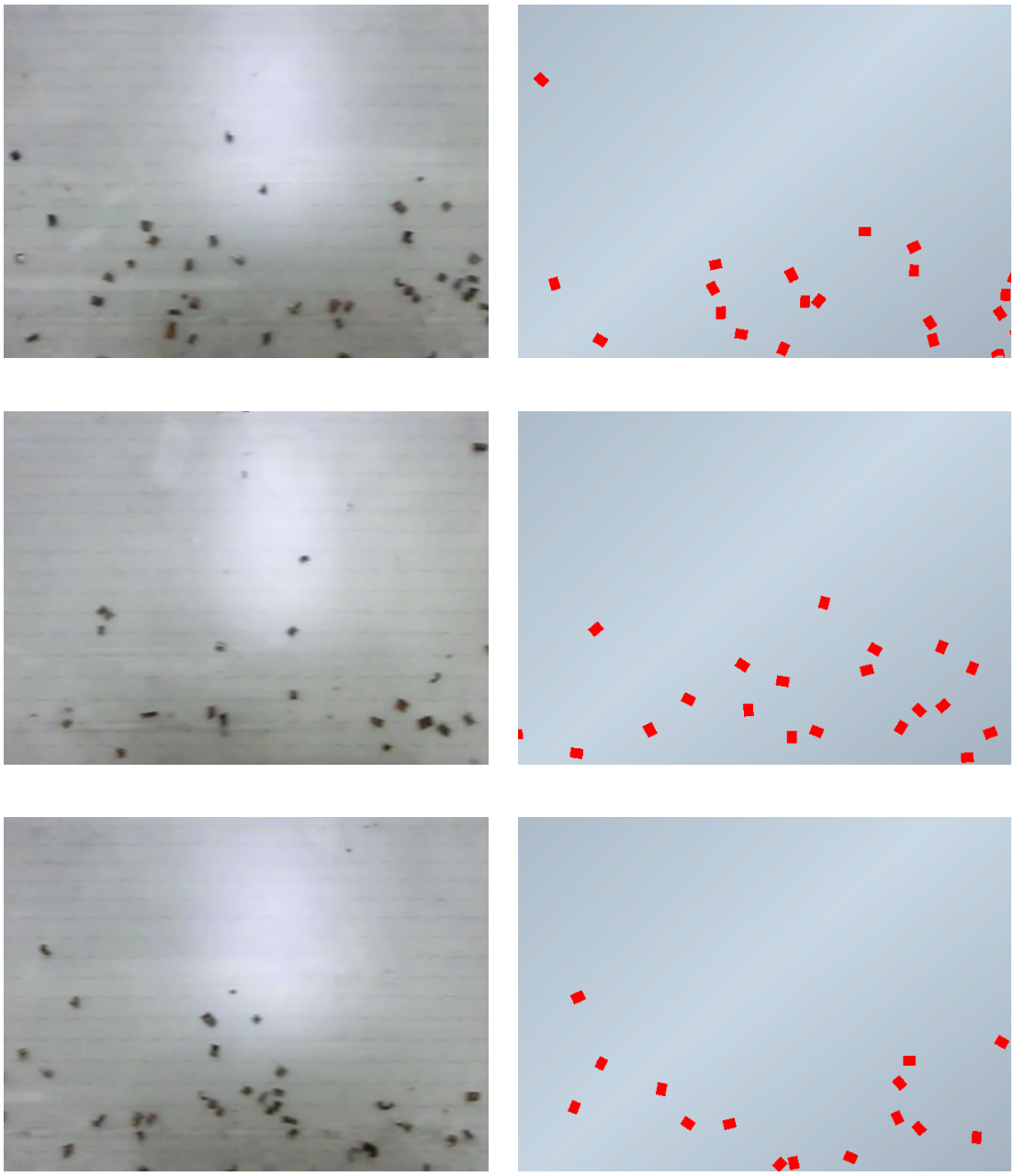

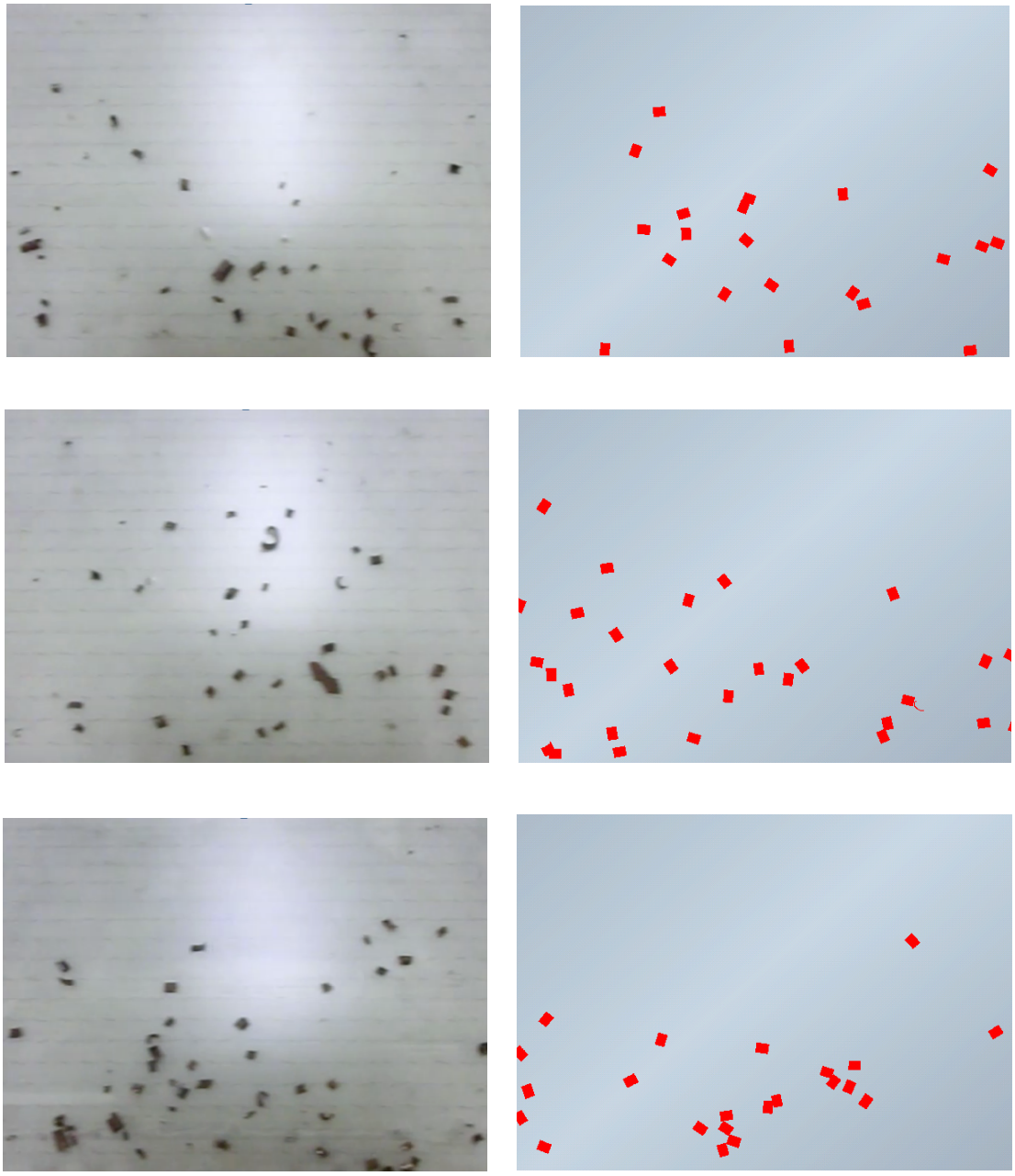

Figure 8: Comparison of experiment images and simulations.

To further validate the model under various conditions, two types of chips, two drum settings, two belt speeds, and two drum speeds were selected and tested. The design of these experiments is shown in table II.

Five feed rates were tested for each set: 10 kg/hr, 20 kg/hr, 30 kg/hr, 40 kg/hr and 50 kg/hr.

Table II: Design of experiments to validate modified model.

Validation experiments	Material	Drum hole size	Belt speed	Drum speed
1	Iron chips	8.33	100	60
2	Iron chips	8.33	100	30
3	Ti-6242 chips	8.33	100	60
4	Ti-6242 chips	10.32	50	60

Simulations were conducted to allow a comparison with the experiments. Chip attributes, including chip morphology, chip density, and chip size distribution were assigned to iron chips and Ti-6242 chips, respectively. Two hole configurations were imported into the model to represent the actual hole sizes: 8.33 mm and 10.32 mm.

The results of the model-predicted belt coverage versus the belt coverage obtained through the experiment are shown in figures 9-12. The data obtained from experiments was averaged from six independent experiments, with each experiment averaged from 20 snapshots.

In all cases, the model shows good agreement with measured belt coverage and throughput rate. It is observed that under each condition, belt coverage was smaller than that measured in the experiment. The reason for this is that the simplified chips have a larger thickness compared to the real chips, which reduces the probability of chips passing through the holes of the drum. Even so, the model is still a reliable predictor of belt coverage.

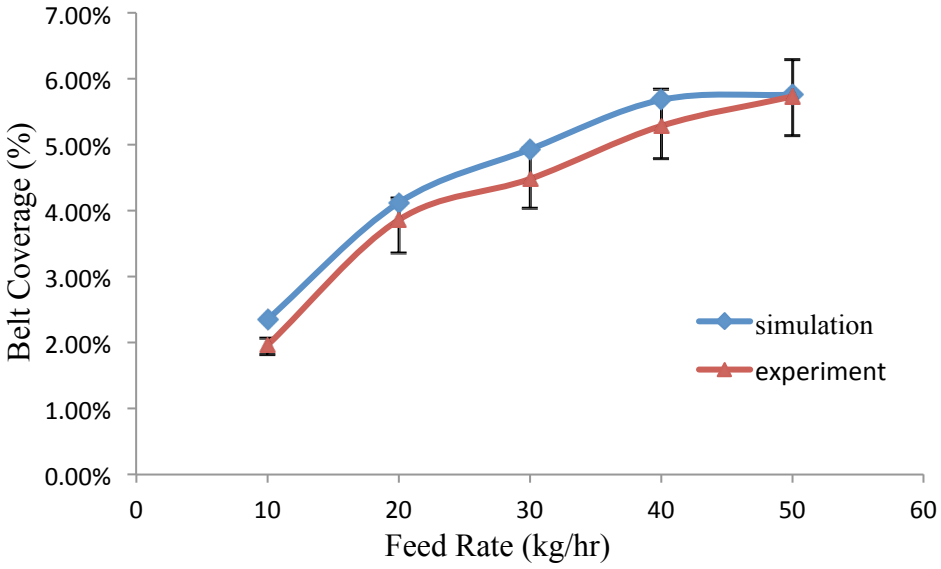

Figure 9: model validation, iron machined chips: 60 RPM, 100 FPM, 8.33 mm.

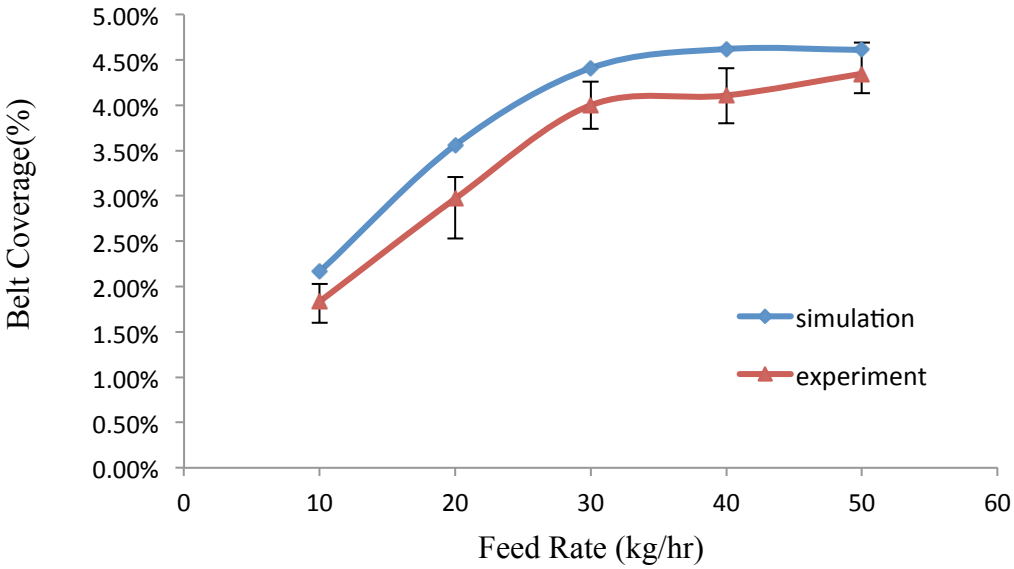

Figure 10: model validation, iron machined chips: 30 RPM, 100 FPM, 8.33 mm.

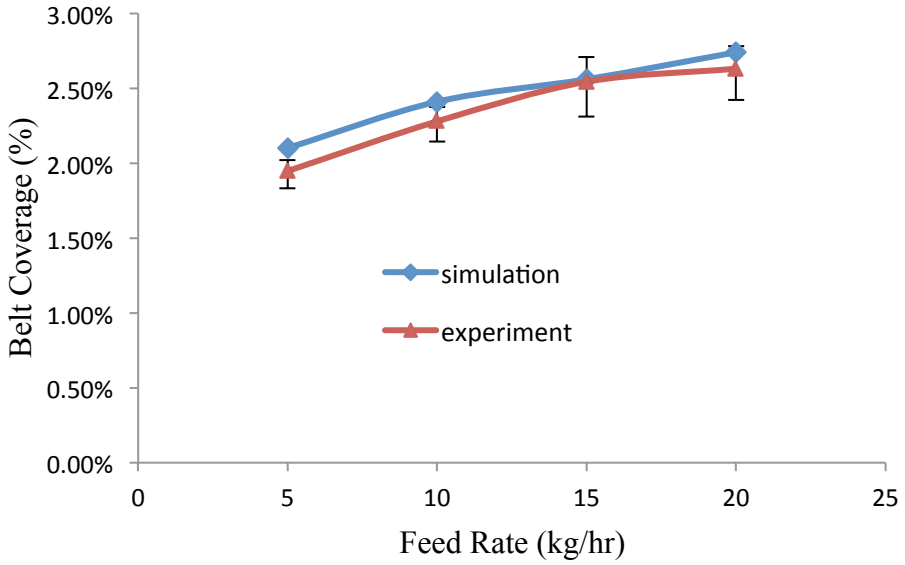

Figure 11: model validation, Ti-6242 chips: 60 RPM, 100 FPM, 8.33 mm.

(a) belt coverage, (b) throughput

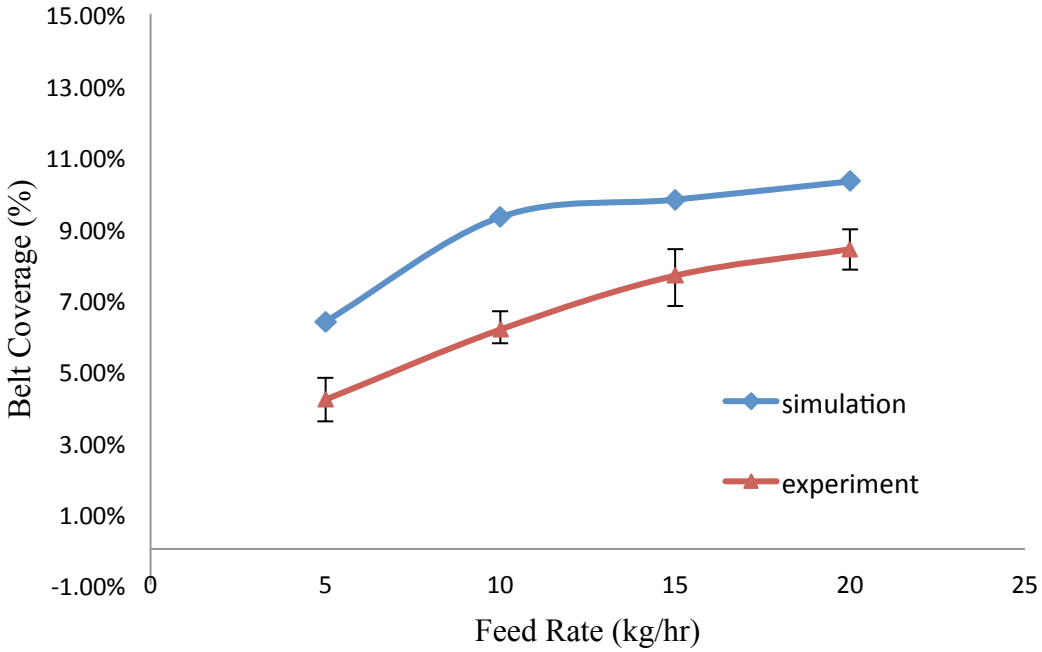

Figure 12: model validation, Ti-6242 chips: 60 RPM, 50 FPM, 10.32 mm.

Conclusions

The success of intelligent sorting relies on the control of chips distribution on the conveyor belt, which is characterized by belt coverage. CRF feeding is a complex process with many variables involved. Considering this, a model was developed using the discrete element method. The developed model was able to simulate the entire feeding process. The model was validated under various conditions and the obtained results show that the model can predict belt coverage accurately.

References

[1] D. B. Spencer, "The High-Speed Identifi cation and Sorting of Nonferrous Scrap," JOM, pp. 46 - 51, Apr 2005.

[2] S. Koyanaka and K. Kobayashi, "Automatic sorting of lightweight metal scrap by sensing apparent density and three-dimensional shape," Resources, Conservation and Recycling, vol. 54, p. 571–578, 2010.

[3] M. Mesina, T. d. Jong and W. Dalmijn, "Automatic sorting of scrap metals with a combined electromagnetic and dual energy X-ray transmission sensor," Int. J. Miner. Process, vol. 82, pp. 222-232, 2007.

[4] S. Zhang, E. Forssberg, B. Arvidson and W. Moss, "Aluminum recovery from electronic scrap by High-Force® eddy-current separators," Resources, Conservation and Recycling, vol. 23, pp. 225-241, 1998.

[5] R. Noll, H. Bette, A. Brysch, M. Kraushaar, I. Monch, L. Peter and V. Sturm, "Laser-induced breakdown spectrometry — applications for production control and quality assurance in the steel industry," Spectrochimica Acta Part B, vol. 56, pp. 637-649, 2001.

[6] R. Noll, V. Sturm, Ü. Aydin, D. Eilers, C. Gehlen, M. Höhne, A. Lamott, J. Makowe and J. Vrenegor, "Laser-induced breakdown spectroscopy:From research to industry, new frontiers for process control," Spectrochimica Acta Part B, vol. 63, pp. 1159-1166, 2008.

[7] T. Pretz and D. Killmann, "Possibilities of sensor based sorting regarding recycling of waste," Acta Metallurgica Slovaca, Vols. 188-193, p. 12, 2006.

[8] R.L.Moss, E.Tzimas, H.Kara, P.Willis and J.Kooroshy, "Critical Metals in Strategic Energy Technologies," European Commission Joint Research Centre, 2011.

[9] M. Buchert, A. Manhart, D. Bleher and D. Pingel, "Recycling critical raw materials from waste electronic equipment," 2012.

[10] W. D. a. H. K. T.P.R. de Jong, "Dual energy X-ray transmission imaging for concentration and control of solids," XXII International Mineral Processing Congres - IMPC, Cape Town, 2003.

[11] T. D. W. de Jong, "X-ray transmission imaging for process optimisation of solid resources," Proceedings R'02 Congress,, 12-15 Feb 2002.

[12] S. E, "Eddy current techniques for segregating nonferrous metals from waste," Conserv, vol. 5, pp. 149-162, 1982.

[13] F. E. Zhang S, "Eddy current separation technology: overview, fundamentals and applications," MIMER Report No. 7.Lulea˚, Sweden: Division of Mineral Processing, Lulea˚ University of Technology, 1997.

[14] R. Wyss and Schultz.P.B, "Color Sorting Aluminum Alloy for Recycling," The Minerals, Metals & Materials Society, pp. 1093-1098, 1999.

[15] J. Kolacz and J. Chmelar, "Cost Effective Optical Sorting System," Recycling and Waste Treatment in Mineral and Metal Processing: Technical and Economic

Aspects, pp. 313-322, 2002.

[16] W. Forsthoff, "Optical Sorting of Coarse Materials," ZKG International , vol. 53, pp. 329-331, 2000.

[17] H. Wotruba and H. Harbeck, "Sensor-Based Sorting," Ullmann's Encyclopedia of Industrial Chemistry., vol. 32, pp. 395-404, 2010.

[18] R. M. H. A. J. F. S. JEFFREY W. SULLIVAN, "THE PLACE OF THE TROMMEL IN RESOURCE," in 1992 National Waste Processing Conference, 1992 National Waste Processing Conference.

[19] S. M. Cleary P.W., "DEM modelling of industrial granular flows: 3D case studies and the effect of particle shape on hopper discharge," Appl. Math. Modell, vol. 26, pp. 89-111, 2002.

[20] S. O. Cundall P.A., "A discrete element model for granular," Géotehnique, vol. 29, pp. 47-65, 1979.

PAPER III

Design of a New Feeding Technology for Feeding Small Metal Chips – Beta Trials

H. Yu and D. Apelian

Center for Resource Recovery and Recycling

Metal Processing Institute

WPI, Worcester, MA 01609 USA

Keywords: Scrap Recycling, Automated Sorting, Feeding, Beta Trial

Abstract

The development in sensing technology has made it possible to detect waste composition in real-time, allowing for the recovery of high-value, critical metals. However, due to low volumes and low industrial fragmentation, the handling of critical metal chips is challenging. At the Center for Resource Recovery and Recycling (CR3), a controlled rotary feeder (CRF) was developed. The CRF enables intelligent sorting by feeding scrap particles in a monolayer and within a controlled distance from each other. Beta site trials of the CRF are reviewed and discussed in this paper.

1. Introduction

Waste recovery and recycling are becoming increasingly more pivotal to a sustainable future for both the ferrous and non-ferrous metal industries [1,2]. With the rapid exhaustion of natural resources and the increasing costs of waste disposal, resource recovery and recycling are becoming critical.

Current waste sortation methods rely on differences in the physical properties of the mixed waste [3-5]. Nothing is known about the chemical composition of the waste in

these processes [6-12]. Sensing technology has developed rapidly over the past few decades and enables intelligent sorting by identifying waste composition in real-time [13-16]. Several automated sorting technologies are commercially available in the market. However, when it comes to high-value, critical metals, metal recovery and recycling is not practiced widely. The reasons are complex, but include low volumes, low industrial fragmentation, as well as a lack of specific technologies for these markets.

A typical automatic sorting system consists of three stages [17]: (i) Feeding mixed waste onto the sensing platform, (ii) Waste composition identification, and (iii) Ejection into identified bins. It is notable that sensing and ejection technologies are pretty advanced. The latest sensing technology is capable of detecting particles as small as 1 mm in diameter, and ejection technology can physically separate waste with high accuracy even at ultra-high speeds. All the three stages contribute to the overall efficiency and accuracy of the sorting task. However, among the three stages, feeding is a prerequisite. The feeding stage is essential in that the success of the sensing and ejection stages depends on the monolayer presentation of mixed waste. Selective sorting cannot be realized without a proper feeding technology. Currently, the situation is that when it comes to small particles, scraps, or other small materials, no proper technology is available that can provide a monolayer of small metal chips.

At the Center for Resource Recovery and Recycling (CR3), a controlled rotary feeder (CRF) was developed. A laboratory-scale prototype was designed and constructed, and the results show that the CRF is as feasible and controllable technology. A model was also developed, and laboratory-scale verifications confirmed that the model is able to simulate the process with high accuracy.

To further verify the CRF, a commercial scale CRF was constructed at wTe Corp, and beta trials were conducted. The purpose of these beta trials was to verify the algorithm that was developed to control the feeding process, as well as to validate the model at a commercial scale. The results of the beta site trials are reviewed and discussed in this paper.

2. Experiments

2.1 Construction of the CRF

A commercial-scale CRF was designed by wTe and CR3. The schematic diagram of the CRF feeder is shown in figure 1. The CRF was comprised of a friction drive assembly, which allowed for easy removal of the drum without tools to clean the screens or make adjustments. The friction force of the drive was adjustable, as was the rotational speed via a VFD. The drum was comprised of three "stages" in a hexagonal layout. The perforated screen panels could be quickly and easily changed to allow for different hole sizes and patterns. The three stages made it possible to run different sizes in the upstream and downstream portions of the drum.

The actual CRF apparatus is shown in figure 2. The dimension of the drum is 24 inches wide and 7.5 inches in diameter. Feed comes into the CRF through the hopper located on the left side of the drum, as shown in figure 2. The conveyor system was 24 inches wide and 100 inches long and was made of urethane. Hole sizes were selected based on the chip size distribution. Perforated screens were supplied by McMaster. Screen sizes ranged from 0.125 inches to 0.5 inches, which allowed for feeding of various chip sizes.

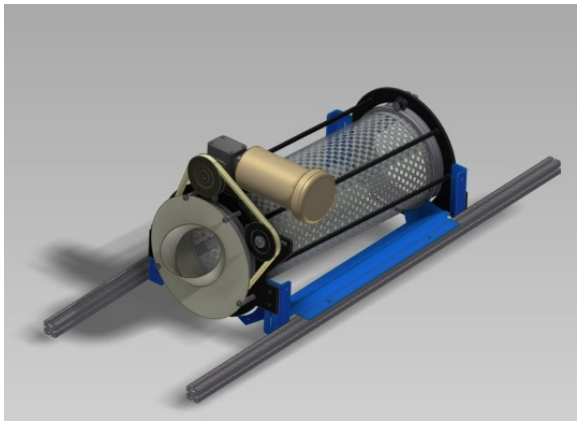

Figure 1: Schematic diagram of commercial scale CRF.

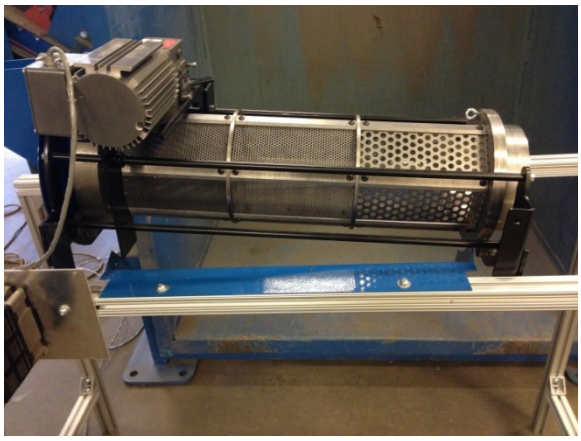

Figure 2: Commercial scale CRF constructed at wTe.

2.2 Materials

Ti-64 chips were selected to conduct the beta trial. Size distribution data for the Ti-64 chips was obtained by a vibrating screener. The results are shown in table I. The majority of the chips were in the range of 2.36 mm to 4.75 mm. The three screen sizes selected for feeding Ti-64 chips were: 3.16 mm, 3.95 mm and 7.9 mm.

Table I: Ti-64 chips size distribution.

Size	Weight (g)	Weight fraction
>5.6 mm	2.528	2.4%
4.75 mm ~ 5.6 mm	3.859	3.6%
2.36 mm ~ 4.75 mm	65.062	61.8%
<2.36 mm	33.836	32.1%

2.3 Experiment procedure

The experiment procedure is summarized in figure 3.

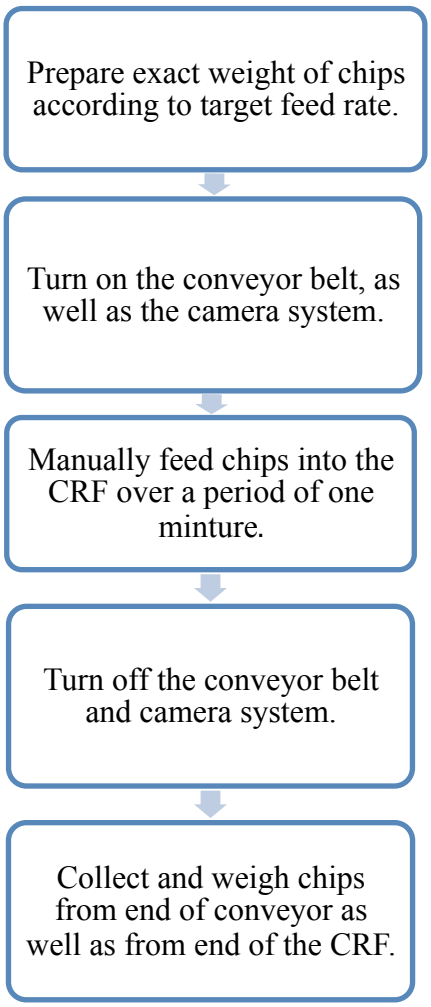

Figure 3: Summary of experiment procedures.

To attain the desired feed rate, feeding was carried out for a one minute period. The exact amount of chips, which was calculated by feed rate (kg/hr) multiplied by feeding time (one minute), was weighed before each experimental run and was tipped into the CRF over a period of one minute. The tipping was controlled to be as smooth as possible to maintain a steady flow rate.

Chips were collected from the end of the CRF, the end of conveyor belt, and the back end of the CRF to calculate throughput rate. Snapshots were extracted from the video footage, and average belt coverage was calculated through the image analysis algorithm.

2.4 Investigated variables

The analysis primarily considered two variables: belt coverage and throughput rate.

Belt coverage is defined as the percentage of belt surface that is covered by a monolayer of chips. As the conveyor was moving at ultra-high speeds, it was impossible to examine belt coverage visually. Therefore, a camera-aided image analysis algorithm was developed.

Videos of chips moving on the conveyor belt were recorded by a high-speed camera, which was placed above the conveyor. The videos were visually inspected and snapshots extracted to analyze the feeding performance. Subsequently, the snapshots were converted into binary images. Belt coverage was obtained in Matlab by calculating the black area of the binary image. Similarly, belt coverage from the simulations was also calculated using Matlab.

A comparison of an image extracted from the feeding video and the converted binary image is illustrated in figure 4.

Throughput rate is defined as the weight of chips coming out the CRF divided by weight of chips fed into the CRF. Throughput rate is a characterization of the CRF's production rate.

Figure 4: Comparison of image extracted from feeding video (left) and converted into a binary image (right).

2.5 Design of experiments

The design of the experiments is shown in Table II.

As the goal of the beta trial was to test the concept of the CRF on a commercial scale, multiple operation parameters were selected and tested.

Four belt speeds were selected: 25 FPM(feet per minute), 50 FPM, 75 FPM and 100 FPM; and two drum speeds were tested for each set of trials: 15 RPM (rounds per minute) and 30 RPM.

Four levels of feed rate were selected for each belt speed. For 25 FPM belt speed, the selected feed rates were 5 kg/hr, 10 kg/hr, 15 kg/hr and 20 kg/hr. For the other three belt speeds, the selected feed rate levels were 10 kg/hr, 20 kg/hr, 30kg/hr and 40 kg/hr.

Table II. Design of experiments for beta trials.

Trial number	Belt speed (FPM)	Drum speed (RPM)	Feed rate (kg/hr)
1	25	15	5, 10, 15, 20
2		30	5, 10, 15, 20
3	50	15	10, 20, 30, 40
4		30	10, 20, 30, 40
5	75	15	10, 20, 30, 40
6		30	10, 20, 30, 40
7	100	15	10, 20, 30, 40
8		30	10, 20, 30, 40

3. Model

The discrete element method (DEM) was used to simulate the process. The commercially available simulation software, EDEM, was selected and used.

3.1 Contact force

In DEM modeling, interactions between the chips, and between the chips and the environment (i.e. rotary feeder and conveyor belt) were calculated and numerically integrated. The Hertz-Mindlin contact force was used to calculate interactions. In Hertz-Mindlin contact mode, the particles are allowed to overlap and the amount of overlap (Δx), and normal and tangential relative velocities determine the collisional forces via Hertz-Mindlin law [18].

The normal force (F_n) is a function of normal overlap (δ) and is given by:

$$F_n = \frac{4}{3} E^* \sqrt{R^*} \delta_n^{\frac{3}{2}}$$

where the equivalent Young's Modulus (E^*) and the equivalent radius (R^*) are defined as:

$$\frac{1}{E^*} = \frac{(1-\nu_i^2)}{E_i} + \frac{(1-\nu_j^2)}{E_j}$$

$$\frac{1}{R^*} = \frac{1}{R_i} + \frac{1}{R_j}$$

with E_i, ν_i, R_i and E_j, ν_j, R_j, being the Young's Modulus, Poisson ratio, and Radius of each sphere in contact.

The tangential force (F_t) depends on the tangential overlap (δ_t) and the tangential stiffness (S_t).

$$F_t = -S_t \delta_t$$

where

$$S_t = 8G^* \sqrt{R^* \delta_n}$$

Here G* is the equivalent shear modulus.

The properties of the Ti-64 chips, the CRF and the conveyor are shown in table III.

Table III: Material properties imported for DEM model.

	Chip density (kg/m^3)	Shear modulus (Pa)	Poisson's ratio
Ti-64 chips	4430	$4e^{+10}$	0.342
Rotary drum	1200	$3e^{+9}$	0.4
Conveyor belt	1100	$1e^{+7}$	0.45

3.2 Model configuration

In EDEM modeling, morphologies of scrap particles are generated by creating complex multi-element particles from simple spherical elements, and merging these

elements into a single particle. The geometries of the CRF and the conveyor belt were generated by Solidworks and imported into EDEM. The imported geometries of the titanium scrap particles and the feeder-conveyor system are shown in figure 5 and figure 6.

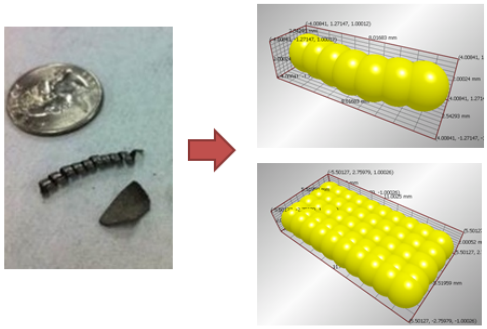

Figure 5: Particle configuration to characterize Ti-64 chips.

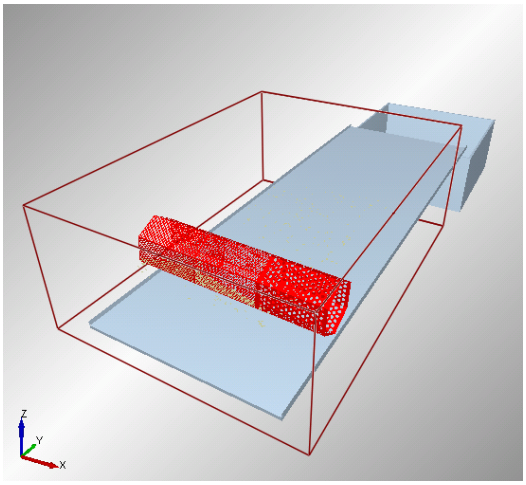

Figure 6: Imported commercial scale CRF geometry.

4. Results and discussion

4.1 Experiments

The beta trial results for belt coverage are summarized in table IV.

A 3-D graph was generated to further illustrate the results. Figure 7 represents variations of belt coverage under various belt speeds and feed rates. It shows that by manipulating belt coverage and feed rate, different belt coverages can be obtained. The graph provides a tool for operators. It can be referred to in order to adjust the

CRF feeding process to obtain the desired belt coverage based on the limitations of sensing and ejection technologies.

Table IV: Summary of beta trial results - belt coverage.

		5 kg/hr	10 kg/hr	15 kg/hr	20 kg/hr
25 FPM	15 RPM	2.43%	4.97%	7.83%	9.05%
	30 RPM	4.07%	8.51%	10.41%	12.36%
		10 kg/hr	20 kg/hr	30 kg/hr	40 kg/hr
50 FPM	15 RPM	2.03%	5.05%	6.68%	8.10%
	30 RPM	3.86%	6.12%	8.36%	10.50%
70 FPM	15 RPM	1.70%	3.20%	5.63%	7.15%
	30 RPM	2.33%	4.93%	6.06%	8.47%
100 FPM	15 RPM	1.43%	2.52%	3.06%	3.87%
	30 RPM	1.91%	3.27%	4.74%	5.40%

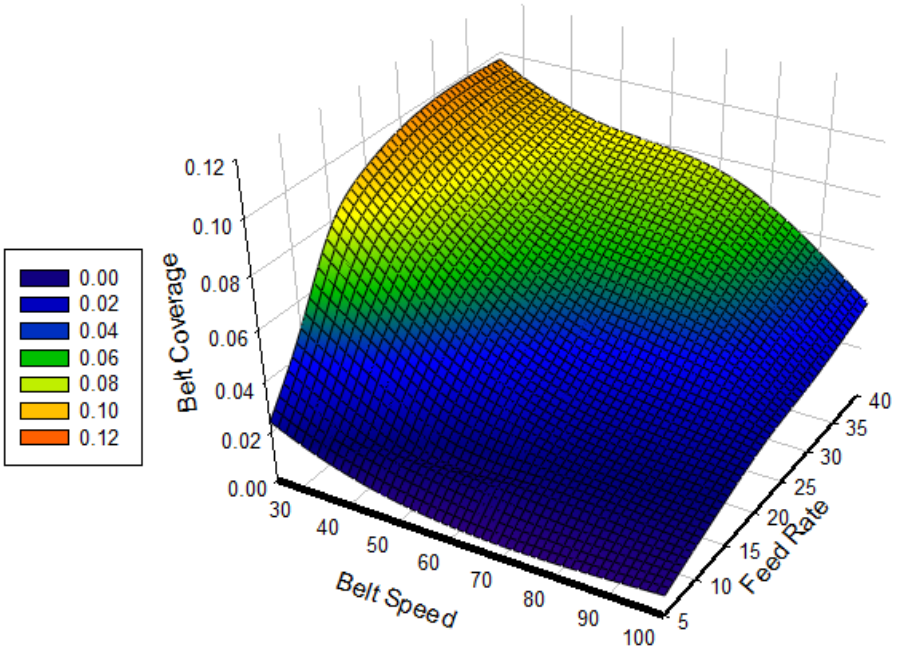

Figure 7: Variations of belt coverage under various operational parameters.

Throughput rates for each trial run are summarized in table V. It can be seen that in most cases throughput rate is higher than 93 percent, indicating that the CRF has excellent productivity.

Table V: Summary of beta trial results - throughput rates.

		5 kg/hr	10 kg/hr	15 kg/hr	20 kg/hr
25 FPM	15 RPM	96.24%	94.92%	96.96%	97.53%
	30 RPM	97.80%	97.86%	97.28%	98.40%
		10 kg/hr	20 kg/hr	30 kg/hr	40 kg/hr
50 FPM	15 RPM	98.58%	98.19%	96.42%	82.59%
	30 RPM	97.20%	99.27%	97.20%	96.11%
70 FPM	15 RPM	97.92%	96.24%	95.40%	84.18%
	30 RPM	96.78%	97.68%	96.62%	95.96%
100 FPM	15 RPM	99.00%	97.56%	95.80%	83.13%
	30 RPM	98.94%	97.98%	97.22%	93.11%

4.2 Model

Comparisons of the experiments and the simulations are shown in figure 8. Belt speed and drum speed were 100 FPM and 30 RPM respectively, and feed rate increased from 10 kg/hr to 40 kg/hr. The images show that as feed rate increases, belt coverage also increases. The simulation is in good agreement with the beta trials.

(a)

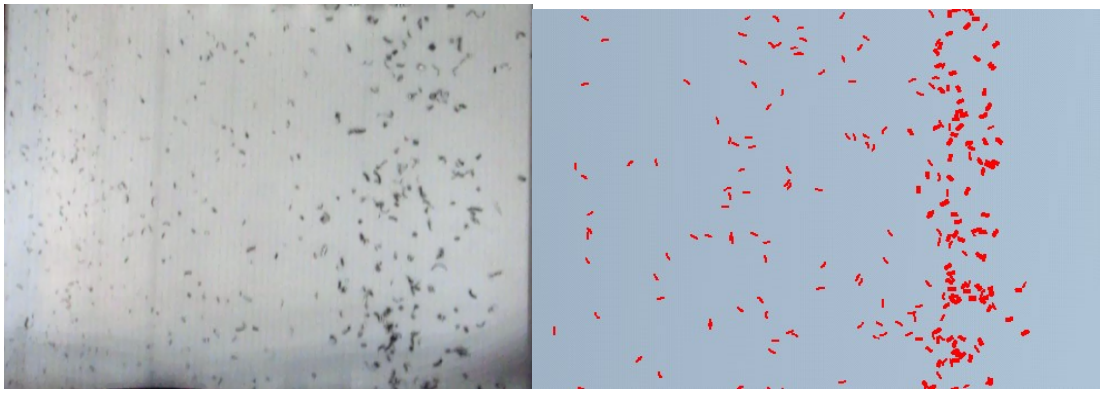

(b)

(c)

(d)

Figure 8. Comparison of chip distribution on the coveyor belt in experiments and in simulations. Belt speed = 100 FPM, drum speed = 30 RPM.
(a) Feed rate: 10 kg/hr; (b) feed rate: 20 kg/hr;
(c) feed rate: 30 kg/hr; (d) feed rate: 40 kg/hr.

Table VI. Comparison of belt coverage and throughput rate in experiment and in simulation.

Belt speed (FPM)	Drum speed (RPM)	Feed rate (kg/hr)	Belt coverage (%)		Throughput rate(%)	
			Experiment	Simulation	Experiment	Simulation
100	30	10	1.91	1.75	98.94	92.23
		20	3.27	2.91	97.98	91.37
		30	4.74	4.06	97.22	90.14
		40	5.40	4.73	93.11	88.09

Table VI presents a comparison of belt coverage and throughput rate in the experiments and the simulations. It shows that although there is a difference between the experiments and simulations, the model is able to predict feeding performance

quite well.

4.3 Discussion

It should be noted that the results for belt coverage and throughput rate in the simulations are smaller than those in the experiments. This is because the accuracy of DEM simulations is dependent on the simulation time-step, which is determined by the Rayleigh time. A number of equations have been proposed for the calculation of a critical time-step. One simplified equation is shown in equation 8 [19].

$$T = \pi * r * sqrt(\rho / \mathrm{G}) / (0.163 * \nu + 0.8766)$$

where r is the radius of the particle, ρ is the density, G is Shear modulus, and v is the Poisson's ratio.

The Rayleigh time-step is a function of element radius, element density, Shear modulus and Poisson ratio. Density, Shear modulus, and Poisson ratio are determined by material attributes. In this application, as the thickness of the single chip particles is smaller than one millimeter, a modified model was used to represent the morphology of single chip particles. Figure 9 represents a comparison between the original model and the modified model to represent particle morphology. The advantage of the modified model is that it can reduce simulation time massively. The accuracy of the simulation can be improved if a better computation device is used.

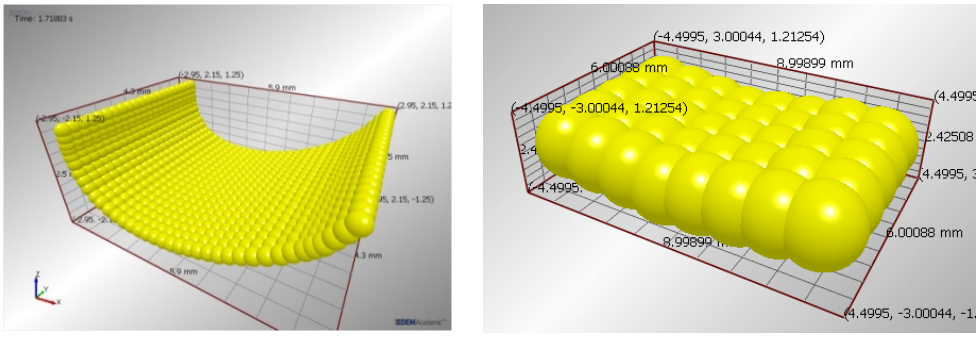

Figure 9: Simplified EDEM particle configuration (original model on left, modified model on right)

Table VII: Simulation computation time before and after simplification.

	Radius of chip element	Number of elements for each chip	Total number of elements for a 10-second simulation	Rayleigh time step (second)	Simulation time
Original model	0.15 mm	780	390,000	$3.7\ e^{-7}$	More than 500 hours
Modified model	1 mm	40	20,000	$7.84\ e^{-6}$	Around 30 hours

5. Conclusions

Beta site trials for CRF feeding were implemented to evaluate its potential for commercialization. The results show that CRF is feasible and controllable at a commercial scale. The developed model was also validated, and the results show that although there were differences between the simulation and the experiment, the model is still able to reliably predict the feeding process.

6. References

[1] R.L.Moss, E.Tzimas, H.Kara, P.Willis and J.Kooroshy, "Critical Metals in Strategic Energy Technologies," European Commission Joint Research Centre, 2011.

[2] M. Buchert, A. Manhart, D. Bleher and D. Pingel, "Recycling critical raw materials from waste electronic equipment," 2012.

[3] "A Review of Optical Technology to Sort Plastics & Other Containers," Environment & Plastics Industry Council, 2008.

[4] H.R.Manouchehri, "Sorting: Possibilities, Limitations and Future".

[5] D. B. Spencer, "The High-Speed Identifi cation and Sorting of Nonferrous Scrap," JOM, pp. 46 - 51, Apr 2005.

[6] S. E, "Eddy current techniques for segregating nonferrous metals from waste," Conserv, vol. 5, pp. 149-162, 1982.

[7] W. Forsthoff, "Optical Sorting of Coarse Materials," ZKG International, vol. 53, pp. 329-331, 2000.

[8] S. Koyanaka and K. Kobayashi, "Automatic sorting of lightweight metal scrap by sensing apparent density and three-dimensional shape," Resources, Conservation and Recycling, vol. 54, p. 571–578, 2010.

[9] M. Mesina, T. d. Jong and W. Dalmijn, "Automatic sorting of scrap metals with a combined electromagnetic and dual energy X-ray transmission sensor," Int. J. Miner. Process, vol. 82, pp. 222-232, 2007.

[10] W. D. a. H. K. T.P.R. de Jong, "Dual energy X-ray transmission imaging for concentration and control of solids," XXII International Mineral Processing Congres - IMPC, Cape Town, 2003.

[11] R. Wyss and Schultz.P.B, "Color Sorting Aluminum Alloy for Recycling," The Minerals, Metals & Materials Society, pp. 1093-1098, 1999.

[12] S. Zhang, E. Forssberg, B. Arvidson and W. Moss, "Aluminum recovery from electronic scrap by High-Force® eddy-current separators," Resources, Conservation and Recycling, vol. 23, pp. 225-241, 1998.

[13] R. Noll, H. Bette, A. Brysch, M. Kraushaar, I. Monch, L. Peter and V. Sturm, "Laser-induced breakdown spectrometry — applications for production control and quality assurance in the steel industry," Spectrochimica Acta Part B, vol. 56, pp. 637-649, 2001.

[14] R. Noll, V. Sturm, Ü. Aydin, D. Eilers, C. Gehlen, M. Höhne, A. Lamott, J. Makowe and J. Vrenegor, "Laser-induced breakdown spectroscopy:From

research to industry, new frontiers for process control," Spectrochimica Acta Part B, vol. 63, pp. 1159-1166, 2008.

[15] U. Habich, "Sensor-Based Sorting Systems in Waste Processing".

[16] H. Wotruba and H. Harbeck, "Sensor-Based Sorting," Ullmann's Encyclopedia of Industrial Chemistry., vol. 32, pp. 395-404, 2010.

[17] H. Wotruba, "State-of-the-art of Sensor-Based Sorting," BHM , vol. 6, pp. 221-224, 2008.

[18] S. O. Cundall P.A., "A discrete element model for granular," Géotehnique, vol. 29, pp. 47-65, 1979.

[19] M. M. J. H. Joanna Sykut, "Discreteelementmethod(DEM) As a Tool Forinvestigating Properties Of Granular Materials," Pol.J.Food Nutr. Sci. , vol. 57, pp. 169-173, 2007.

PAPER IV

Automated Metal Sortation

H. Yu and D. Apelian

Center for Resource Recovery and Recycling

Metal Processing Institute

WPI, Worcester, MA 01609 USA

Keywords: Critical Metals, Scrap Recycling, Automated Sorting, Feeding

Abstract

Waste recovery and recycling is important to mitigate the effects of growing global material consumption, especially in the metal industry. The first step in waste recovery is to sort waste mixtures into different types. Waste sortation has been practiced for many years. Recent developments are providing us with technologies that allow us to identify mixed waste based on the chemical composition of the feed - techniques such as X-ray Fluorescence (XRF), which the chemical composition of metals or alloys to be determined in real-time. This opens a vista of opportunities to upgrade the value of waste streams by intelligently separating out unwanted materials leaving only the desired alloys, and identifying a specific alloy within a mixture of alloys. In this paper, the development of a potential new waste sortation system is reviewed.

1. Introduction

In recent years, waste recovery and recycling have become increasingly more pivotal to a sustainable future for both the ferrous and non-ferrous metal industries [1,2]. With the exhaustion of natural resources and increasing waste disposal costs, resource recovery and recycling are becoming critical. Figures 1 and 2 below show the annual production of key metals, as well as the ore grade for these metals. It is clear that

production is increasing dramatically, whereas the ore grade is decreasing over time, further confirming the critical importance of resource recovery and recycling.

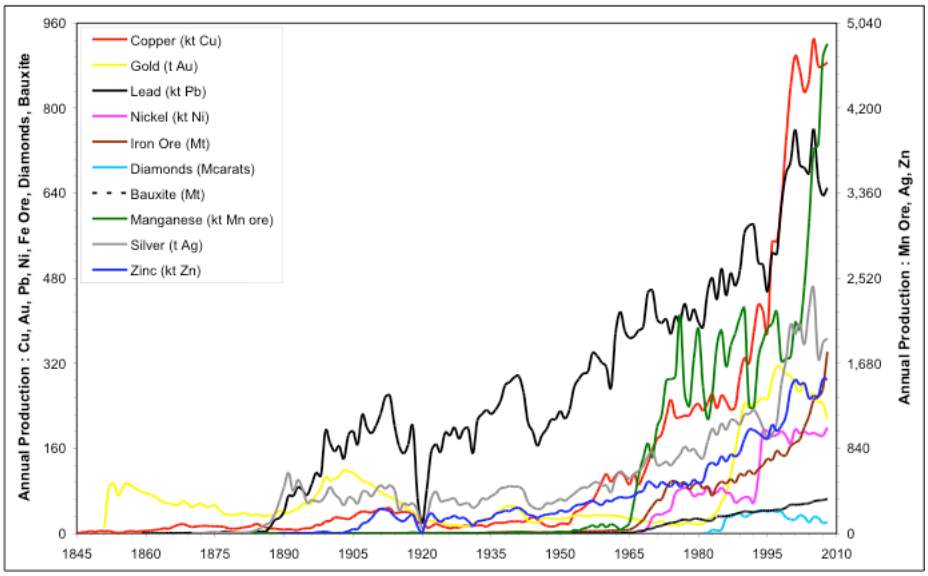

Figure 1: Annual production of key metals over time [3].

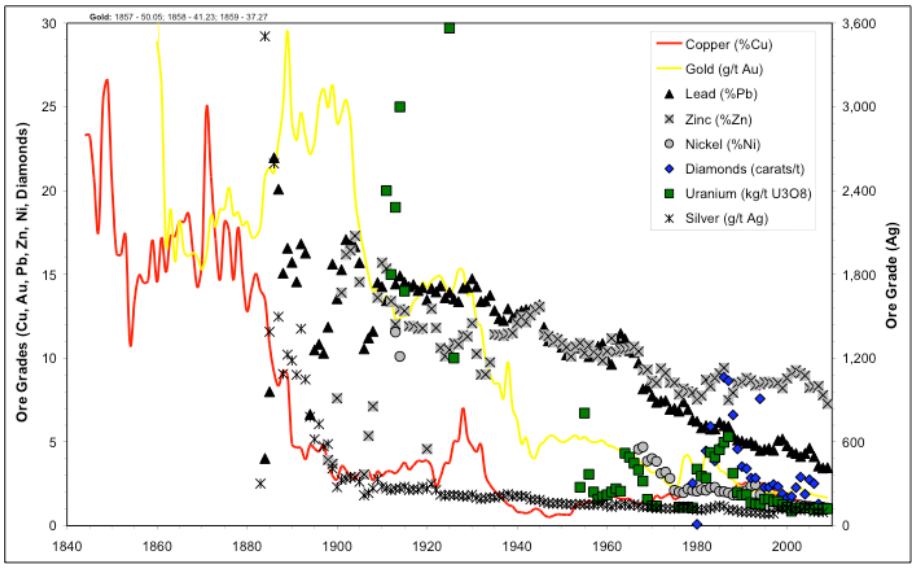

Figure 2: Ore grade as a function of time for key metals [3].

In this context one would imagine that the rate of metal recycling would also have increased dramatically over the past decades, however, the facts do not suggest that this is the case.

Figure 3 is a summary of the recycling rates for sixty metals. It can be noticed that only less than one third of the metals have a recycling rate higher than 50 percent. In the meantime, more than half of the metals are being recycled at a rate of less than 1 percent. Based on this, it is clear that much work needs to be done for the metal recycling industry to improve the rates of waste metal recovery.

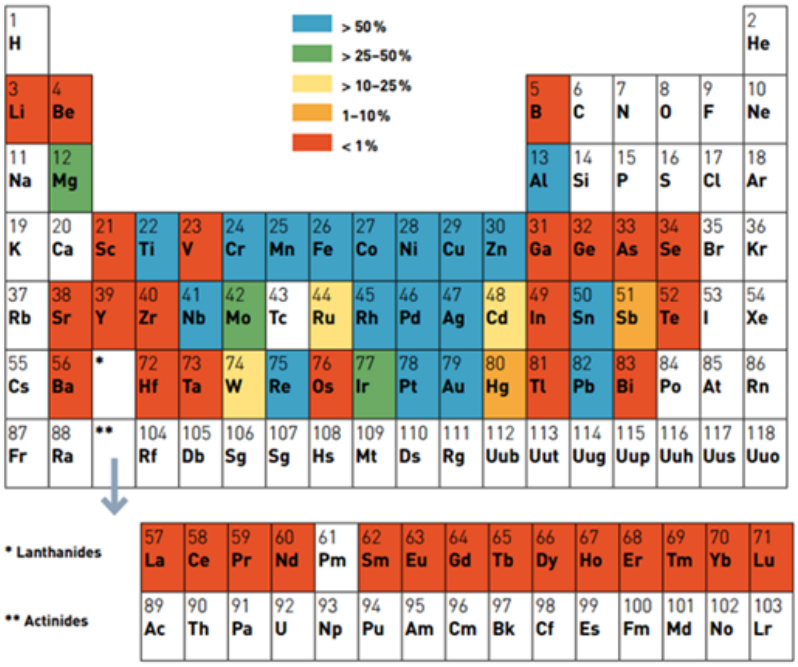

Figure 3: Recycling rate for sixty metals [4].

Another fact that can be seen from figure 3 is that the more the metal is used, the higher its rate of recycling. Metals with a 50 percent or higher recycling rate include iron, aluminium, copper, and zinc, which are commonly used in the manufacture of automobiles, electronics, and home supplies. For example, aluminum, which is a major component in cars, cans, planes, and window frames, has an annual consumption of 20.3 kg per capita. Therefore, the recycling rate of aluminum is high: nearly 75 percent of aluminum produced since the 19th century is still in use today [5].

Besides these structural metals, there are other metals, including tantalum, tungsten, molybdenum, zirconium, and niobium, which are valuable and of critical importance to the manufacturing industry, but are in short supply [6]. These metals are referred to as critical metals. For example, tantalum has a wide range of applications: It is used in

the manufacture of electronic capacitors for electronic applications, such as mobile phones and computers; it is used as an alloying element in superalloys for the aerospace industry; and it is a key component in metal products for the medical, pharmaceutical, and chemical industries [7]. All of these applications make tantalum a pivotal metal element.

However, critical metals are being recycled at a low rate. The reasons for this are complex, but include low volumes, industry fragmentation, as well as lack of specific technologies for these markets.

The most notable feature for critical metals is their low volume in manufactured products. Morphologies of shredded end-of-life cell phones and aerospace superalloy scraps are shown in figure 4. It can be seen that shredded end-of-life cell phones are presented in the form of very fine scraps, while aerospace waste takes the form of small scraps. It is extremely difficult to process and sort these types of waste: a special sorting technology is needed.

Figure 4: Shredded cell phone [8] and aerospace superalloy scrap. [9]

2. Sorting technologies

Based on working principles, sorting technologies can be grouped into three categories: hand picking, physical sorting technologies, and sensor-based sorting technologies.

Hand picking is the oldest sorting technique with a history dating back to ancient times [9]. Workers manually sort mixed waste based on criteria such as color, density, and morphology. The potential of hand sorting is limited by low accuracy, low productivity, and labor intensiveness. Nevertheless, it is still practiced in small-scale sorting facilities and is the main method for sorting non-ferrous metals.

Later, technologies utilizing physical properties emerged and were widely adopted [10-15]. These technologies include heavy-media separation, magnetic separation, and eddy current separation.

2.1 Heavy-media separation

Heavy-media separation is one of the oldest technologies in mineral processing to separate particulate solids of different densities in a mixture [16]. The process usually involves using a mixture of fine media material, such as magnetite or ferrosilicon, suspended in a slurry of water, to produce a media slurry with a specific gravity that will allow low density materials to float, and other high density materials to sink [17].

2.2 Magnetic separation

Magnetic separation is a sorting technology in which the magnetic susceptibility of the waste scraps is measured [18].

When large quantities of ferrous scraps are to be sorted out from other materials, magnetic separation is often the first choice. The basic principle of magnetic separation is that when materials pass near magnets, ferrous materials attach to the magnets and are thereby extracted, while non-ferrous materials do not [19]. Two types

of magnets are commonly used: permanent magnets and electromagnets [16]. The separation system can either be a belt-type or drum-type system. In the drum-type system a permanent magnet is located inside a rotating shell, and materials pass under the drum on a belt. A belt-type separator is similar, except that the magnet is located between pulleys around which a continuous belt travels.

Figure 5 is a schematic representation of a drum magnetic separator. Mixed materials are fed in through the top where a revolving cylinder carries them over a stationary magnet. The magnetic field attracts and holds magnetic scraps and releases them near the far edge of the drum, while non-magnetic materials fall past it due to the force of gravity.

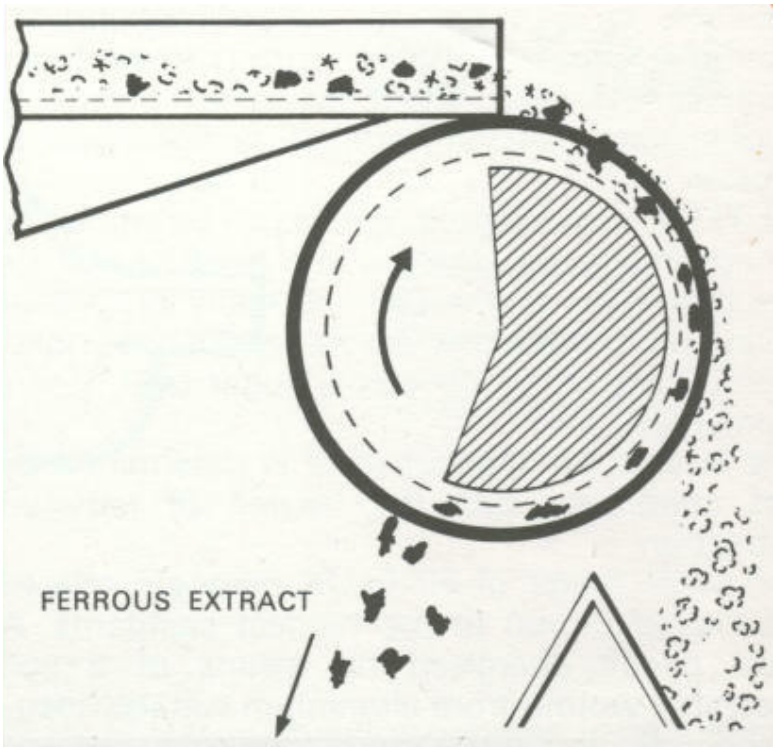

Figure 5: Schematic representation of drum magnetic separation [20].

Magnetic separation is cost effective and operationally easy, which is why it is widely used in mineral sorting and metal recovery. However, the main drawback of this technique is that it cannot separate different magnetic scraps, for example, iron and steel from nickel, meaning its application is limited.

2.3 Eddy current separation:

Eddy current separation is based on the electrical conductivity differences of the waste materials [10]. This technique is used to separate metals from non-metallic materials. For example, aluminum can be separated from glass using the eddy current separation method. Gravity separation is not an option because the difference in the densities of the two materials is very small.

The principle of eddy current separation is illustrated in figure 6. The feed is carried by a conveyor belt into an alternating magnetic field that is produced by a high speed cylindrical assembly of permanent magnets rotating inside an outer drum. The feed materials leave the conveyor belt in various streams: non-ferrous metals are accelerated away far from the drum due to the eddy current generated; non-metallic scraps drop near the drum with gravity; and ferrous metals are attached to the drum and brushed off [16].

Eddy current separation has been applied for non-ferrous metal recovery from auto-shredder residue. After steel is extracted from shredded automobile scrap, the remaining waste includes glass, plastic, rubber, grit and dirt. The metals recovered are mainly zinc and aluminum alloys with smaller amounts of magnesium, copper, stainless steel, lead, and iron that were not successfully separated.

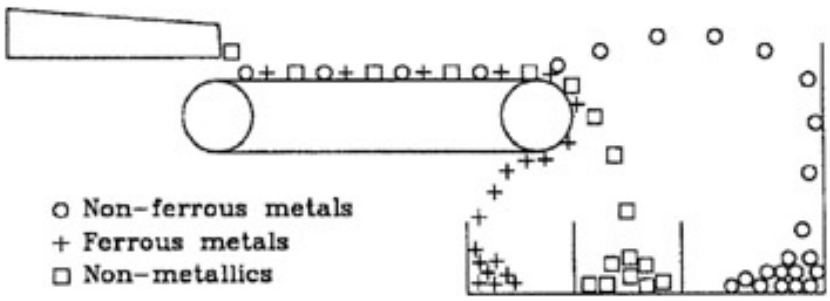

Figure 6: Principle of an eddy current separator [21].

3. Sensor based sorting

In recent decades, with the development of sensing technologies and robotic waste handling, automated sorting has been widely applied [22-26]. In this process, the

chemical composition of waste is detected by sensing systems. This has made it possible to sort all types of metals, even alloys, intelligently.

In sensor-based sorting processes, waste mixtures are introduced into the sorting system in a one-by-one form, allowing every single waste scrap to be scanned by a sensor. Information is obtained and transmitted to a computer, a yes/no decision is made and transmitted to trigger a mechanical separation device [25].

A typical automatic atomic sortation system consists of three steps [26]: (i) Feeding mixed waste onto the sensing platform, (ii) Waste composition identification, and (iii) Ejection into identified bins.

The purpose of the feeding stage is to present waste materials to the sortation system. The waste must be presented in such a manner that the scraps do not overlap or lie on top of each other, and that there is enough space between them so that the sensor and ejector can identify each scrap individually.

Waste identification is the stage in which sensing, or identification, is carried out. In this step, every single piece of waste is scanned. Information about the waste's composition is processed through a computer and transmitted to the rejecter.

Physical separation is the third stage. The ejection device is triggered when a contamination is discovered by the sensor. Multiple ejection techniques can be used, but air gun ejection, mechanical ejection and water ejection are the most common [22].

A large number of different sensing technologies can be applied, including color sensors, X-ray transmission sensors, laser-induced breakdown spectroscopy sensors, and X-ray fluorescence sensors [27-32].

3.1 Color sorting

Color sorting is a technique that relies on differences in the surface colors of the mixed waste. It is widely used in glass and plastic sorting [27].

The color sorting system normally consists of an illumination unit and a color camera, or, more commonly, a linear arrangement of single camera detectors [26]. The objects move toward the camera at a constant speed and are scanned in a single line. Each of the measure lines is then put together to form a two-dimensional image.

In metal recycling, color sorting is usually used as a subsequent step for the recycling of shredded metals after magnetic separation, eddy current separation, or X-ray separation, after which the remaining metals form a mixture of heavy non-ferrous metals, such as copper (red), brass (yellow), and zinc or stainless steel (grey).

The accuracy of this technique can be as high as 95 percent, and a flow rate of more than 10 tons per hour is attainable. The resolution limit of color sorting is approximately 5 mm [23].

Color sorting is a surface sensitive technique, meaning coating or surface contamination can cause errors in detection. However, in metal recycling, after the metals have passed through the shredding stage, color sorting can be used to remove metals with surface coating so that metals with uncoated surfaces can be observed in a later sorting stage.

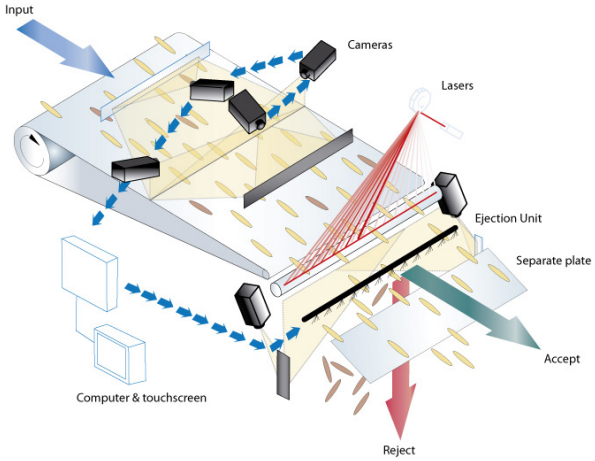

Figure 7: Schematic representation of a color sortation system [33].

Figure 7 shows the setup of a color sortation system. The system consists of four components: a conveyor belt that transports the bulk material, a camera that detects the color of the waste scraps, a data processing system to process signals, and a

pneumatic valve setup to physically separate the materials. Several factors need to be considered here. For example, the background color should match the color of wanted materials as closely as possible. The light source has to be adapted to give enough light for all scraps to be inspected. Moreover, the number, position and width of the pneumatic valves must be electronically set so that the proper valve is always operated.

3.2 X-ray transmission technology

X-ray transmission is a useful and widely used identification technology, especially for high-speed recognition of materials [29-30]. An X-ray transmission beam has a higher intensity than an induced fluorescent beam, making it possible to record images in a matter of milliseconds. This makes X-ray transmission commercially viable for high-speed identification. The resolution limit of this technique is about 2 mm and a conveying speed of over 1 meter per second possible. Another advantage is that with this technology, an X-ray beam is transmitted through the material and the signal is collected at the bottom. This way the material's volume can be detected, not just a surface layer, which provides information about the entire material. The main disadvantage of this method is that no information of the specific phase can be detected. However, monochromatic X-ray transmission can be used for structural identification and contamination examination.

When an X-ray beam interacts with a piece of scrap metal, some of its energy may be absorbed by the metal. The incident beam can still be detected and will transmit the volume of the material. By analyzing the transmitted beam, information about the atom can be acquired.

However, according to Lamber's Law [16], the absorption of X-rays not only depends on the property of the material, but also relies on its thickness. In order to calculate the linear damping coefficient, the thickness of target materials must be known in

advance, which is not realizable in metal recycling since the size and shape of the mixed materials is irregular and not identical.

Dual energy X-ray transmission [34], also known as dual-emission X-ray absorptiometry, is a modified X-ray transmission technique. In this process, two X-ray beams with different energy levels are applied to the material and the transmitted X-ray beams are detected and analyzed using Lamber's Law. Since two X-ray beams are transmitted through the sample, two different sets of data are collected. Therefore, the influence of thickness on the recorded intensity can be eliminated and the absorption coefficient of the material is obtained. This technique was first used for clinical purposes, such as measuring bone mineral density. More recently, researchers have proved that this technique can also be applied in the recycling industry, for example, for the identification and sorting of scrap metals and plastics.

3.3 Laser-induced breakdown spectroscopy

Laser-induced breakdown spectroscopy (LIBS) has advanced significantly in the past few years [31,32]. A typical LIBS system consists of four major components: a neodymium doped yttrium aluminum garnet (Nd:YAG) solid state laser; a wide spectral range spectrometer; a fast, high-sensitivity detector; and a data analysis computer [35].

Like other spectroscopic techniques, LIBS uses a high-energy laser pulse as its excitation source. The laser is focused on a small area on the surface of the specimen. When the laser is discharged, it ablates a small quantity of the surface material (usually in the range of nanograms to picograms) [36], generating a plasma plume with a temperature of about 10,000 – 20,000 Kelvin. At this extremely high temperature, the ablated material breaks down into excited ionic and atomic species, and the plasma emits continuous radiation containing no useful information about the species investigated. However, within milliseconds, the plasma expands at supersonic

velocities and cools down rapidly. At this point the characteristic atomic emission lines can be collected and analyzed.

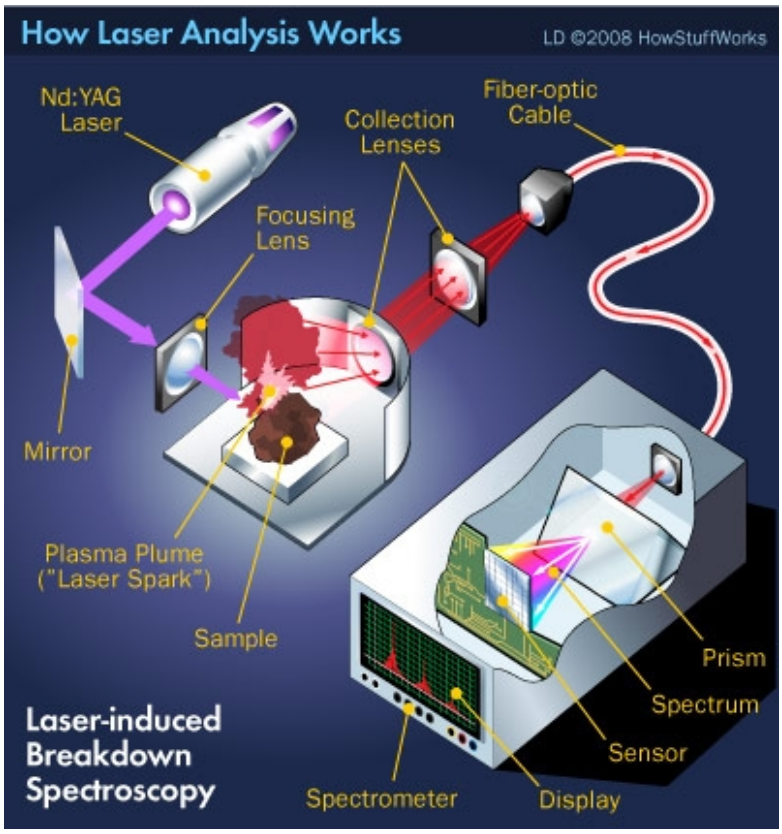

Figure 8: Working principal of laser-induced breakdown spectroscopy [36].

The most significant advantage of LIBS is that it is capable of analyzing any matter regardless of its physical state. Because all elements emit light when excited to sufficiently high temperatures, LIBS can detect all elements in any physical state - solid, liquid or gaseous - as long as the laser is powerful enough to produce a high temperature.

In the LIBS process, the laser can be focused on a very small area of the sample surface, which indicates that only a small amount of material is consumed during the LIBS process. Therefore, LIBS can essentially be considered as a non-destructive technique. Because of this, sample preparation can be minimized or even neglected.

Another major advantage of LIBS is its ability to profile the depth of a specimen by repeatedly discharging the laser in the same position, effectively going deeper into the specimen with each discharge. This technique can also be used to remove surface

contamination, in which the laser is discharged for some time prior to the analysis shot. LIBS is also a very rapid technique giving results within seconds, making it particularly useful for high volume analyses or on-line industrial monitoring.

Like all other analytical techniques, LIBS has limitations. First, it is subject to variations in the laser spark and resultant plasma, which often limits reproducibility. In addition, the complexity and cost of the apparatus limits its application.

3.4 XRF

When an incident X-ray photon of sufficient energy interacts with an atom, its energy can be absorbed through the ejection of an inner shell electron. This reaction, termed "the photoelectric effect", creates an electron vacancy and an ejected photoelectron, but also destabilizes the atom [37]. In this reaction, a more loosely bound electron will fill the electron vacancy with the simultaneous emission of an X-ray photon, or Auger electron, from an outer electron shell. The emitted fluorescent X-ray photon will have a characteristic energy equal to the difference in binding energies between the shell of the transitioning electron and the shell of the vacancy. These characteristic X-rays serve as the "fingerprint" for XRF analysis given that each element has a unique spectrum of electron energy levels and therefore fluorescent X-ray photon energies.

In XRF spectrometry, fluorescent characteristic energy is used for quantitative analysis. The equation below is used to describe the intensity of element i, which uses fundamental parameters [38].

The setup of XRF instrumentation is quite simple and generally consists of four components: an excitation source, a sample, a detector, and a data collection and analysis system.

The excitation source is typically an X-ray tube, but a radioactive isotope may also be used. The X-ray tube sends a beam of X-rays with various energies to the sample, and the sample absorbs and emits the X-rays to the detector. The detector senses each successive X-ray and sends electrical pulses to the data collection and analysis system.

The system categorizes each X-ray by its energy. Then, the data are collected and stored, usually in a computer (Figure 16).

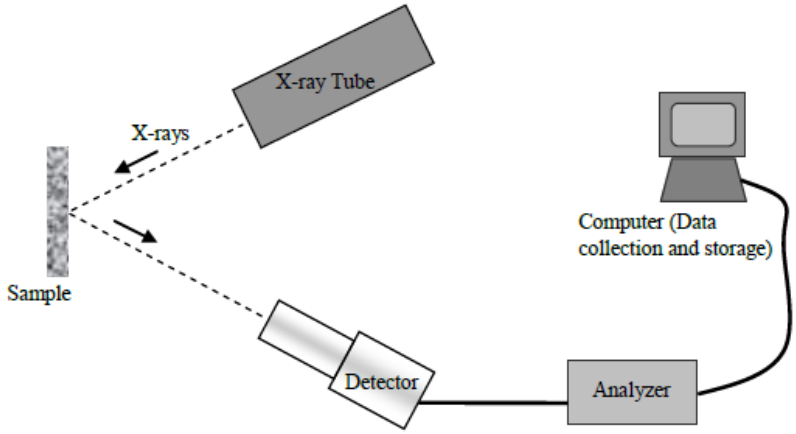

Figure 9: The components of a basic XRF instrumentation setup [39].

XRF is considered a non-destructive testing method with limited or even no sample preparation, which speeds up the process and creates a more efficient process. Moreover, recent advances in XRF have resulted in the development of a portable XRF instrument, which facilitates the test in real-time.

However, since XRF measurements rely on quantity, there are limits on the measurements. The normal quantitative limit is 10 to 20 ppm (parts per million), usually the minimum particles required for an accurate reading. Also, XRF cannot be used to determine beryllium content, which is a distinct disadvantage when measuring alloys or other materials that may contain beryllium.

4. References

[1] R.L.Moss, E.Tzimas, H.Kara, P.Willis and J.Kooroshy, "Critical Metals in Strategic Energy Technologies," European Commission Joint Research Centre, 2011.

[2] M. Buchert, A. Manhart, D. Bleher and D. Pingel, "Recycling critical raw materials from waste electronic equipment," 2012.

[3] G.Mudd, "The Sustainability of Mining in Australia: Key Production Trends and Their Environmental Implications for the Future," 2009.

[4] T. Graedel, J. Allwood, J.-P. Birat, B. Reck, S. Sibley, G. Sonnemann, M. Buchert and O. Hageluken, "Recycling Rates of Metals - A Status Report, A Report of the Working Group on the Global Metal Flows to the International Resource Panel," UNEP, 2011.

[5] T. A. Association, "Aluminum: The Element of Sustainability, A North American Alunimun Industry Sustainability Report," The Aluminum Association, September 2011.

[6] C. Hagelüken and C. E. M. Meskers, "Complex Life Cycles of Precious and Special Metals," Strüngmann Forum Report, Linkages of Sustainability, 2010.

[7] L. Cunningham, "Tantalum recycling in the United States in 1998," USGS Circular, 2004.

[8] J. Neira, L. Favret, M. Fuji, R.Miller, S. Mahdavi and V.D.Blass, "End-of-Life Management of Cell Phones," A Group Project submitted in partial satisfaction of the requirements for the degree of Master's of Environmental Science and Management for the Donald Bren School of Environmental Science and Management.

[9] D. B. Spencer, "The High-Speed Identifi cation and Sorting of Nonferrous Scrap," JOM, pp. 46 - 51, Apr 2005.

[10] S. E, "Eddy current techniques for segregating nonferrous metals from waste," Conserv, vol. 5, pp. 149-162, 1982.

[11] W. Forsthoff, "Optical Sorting of Coarse Materials," ZKG International , vol. 53, pp. 329-331, 2000.

[12] S. Koyanaka and K. Kobayashi, "Automatic sorting of lightweight metal scrap by sensing apparent density and three-dimensional shape," Resources, Conservation

and Recycling, vol. 54, p. 571–578, 2010.

[13] M. Mesina, T. d. Jong and W. Dalmijn, "Automatic sorting of scrap metals with a combined electromagnetic and dual energy X-ray transmission sensor," Int. J. Miner. Process, vol. 82, pp. 222-232, 2007.

[14] F. E. Zhang S, "Eddy current separation technology: overview, fundamentals and applications," MIMER Report No. 7.Lulea˚, Sweden: Division of Mineral Processing, Lulea˚ University of Technology, 1997.

[15] S. Zhang, E. Forssberg, B. Arvidson and W. Moss, "Aluminum recovery from electronic scrap by High-Force® eddy-current separators," Resources, Conservation and Recycling, vol. 23, pp. 225-241, 1998.

[16] S.R.Rao, Resource recovery and recycling from metallurgical wastes, 2006.

[17] E. Pryor, "Dense Media Separation," in Mineral Processing, 1965.

[18] H. K. C. d. E. M. J. O. D. Kelland, "High Gradient Magnetic Separation: An Industrial Application of Magnetism," in Superconducting Machines and Devices , 1974.

[19] J. Svoboda, Magnetic Techniques for the Treatment of Materials, 2004.

[20] C. B. Gill, "Magnetic Separation," in Materials Beneficiation, 1991.

[21] M. Kutz, Environmentally conscious mechanical design, 2007.

[22] H.R.Manouchehri, "Sorting: Possibilities, Limitations and Future".

[23] U. Habich, "Sensor-Based Sorting Systems in Waste Processing".

[24] T. Pretz and D. Killmann, "Possibilities of sensor based sorting regarding recycling of waste," Acta Metallurgica Slovaca, Vols. 188-193, p. 12, 2006.

[25] H. Wotruba, "State-of-the-art of Sensor-Based Sorting," BHM , vol. 6, pp. 221-224, 2008.

[26] H. Wotruba and H. Harbeck, "Sensor-Based Sorting," Ullmann's Encyclopedia of Industrial Chemistry., vol. 32, pp. 395-404, 2010.

[27] "A Review of Optical Technology to Sort Plastics & Other Containers," Environment & Plastics Industry Council, 2008.

[28] J. Kolacz and J. Chmelar, "Cost Effective Optical Sorting System," Recycling and Waste Treatment in Mineral and Metal Processing: Technical and Economic Aspects, pp. 313-322, 2002.

[29] W. D. a. H. K. T.P.R. de Jong, "Dual energy X-ray transmission imaging for concentration and control of solids," XXII International Mineral Processing Congres - IMPC, Cape Town, 2003.

[30] T. D. W. de Jong, "X-ray transmission imaging for process optimisation of solid resources," Proceedings R'02 Congress,, 12-15 Feb 2002.

[31] R. Noll, H. Bette, A. Brysch, M. Kraushaar, I. Monch, L. Peter and V. Sturm, "Laser-induced breakdown spectrometry — applications for production control and quality assurance in the steel industry," Spectrochimica Acta Part B, vol. 56, pp. 637-649, 2001.

[32] R. Noll, V. Sturm, Ü. Aydin, D. Eilers, C. Gehlen, M. Höhne, A. Lamott, J. Makowe and J. Vrenegor, "Laser-induced breakdown spectroscopy:From research to industry, new frontiers for process control," Spectrochimica Acta Part B, vol. 63, pp. 1159-1166, 2008.

[33] T. S. Solutions, Genius optical sorter product report.

[34] S. M. O. R. Ch. Bokun, "Generalization of dual-energy method for material identification with X-ray introscopy," Journal of Surface Investigation. X-ray, Synchrotron and Neutron Techniques, vol. 4, pp. 591-593, 2010.

[35] W. Dalmijn, "Lasers target aluminium alloy sorting," Recycling International,

pp. 48-51, 2003.

[36] W. Harris, "How Laser Analysis Works," 2008.

[37] G. L. Hendry, "X-ray Fluorescence," in Physicochemical Methods of Mineral Analysis, 1975.

[38] L. C.Duren, "X-ray fluorescence measurements of molten aluminum elemental composition".Master Thesis.

[39] B.L.Francom, X-ray Fluorescenece Instrument Calibration: Theory and Application.

APPENDIXES

Appendix A: Matlab Based Code to Calculate Belt Coverage

```
clc; clear all; close all;

% read images and covert to binary

str='G:\beta trial images\100 FPM\30 RPM\40 kg\simulation\'; %% set file
location

%%%%%%%% select max file number

N = 20;

%%%%%%%%

BeltCoverage = [2,N];


for i=1:N

  im=imread([str,num2str(i),'.png']); %% read image
  bg = imread ('bg.png');            %% read background
  [nr,nc,nd] = size(im);             %% read image size


  ip = imsubtract (bg,im);           %% subtract background

  BW = im2bw(ip, 0.1);               %% turn into binary

  BW2 = 1-BW;

   figure;
   imshow(BW2);

  total = bwarea(BW);                %% calculate belt coverage
  area = total/(nr*nc);

  BeltCoverage (1,i)= i;
  BeltCoverage (2,i)= area;

End
```

Appendix B: Matlab Based Code to Calculate Average Chip Distance

```
clc; clear all; close all;

% read images and covert to binary
im = imread('8.tif');
[nr,nc,nd] = size(im);
figure
imshow(im)

BW = im2bw(im, 0.5);
BW2 = 1-BW;

figure
imshow(BW2)

% find small particles and turn into white
BW_inv = bwareaopen(BW2, 50);
imshow(BW_inv);


% label particles
L = bwlabel(BW_inv);

%particle total number
PN = max(max(L))

% get boundary and particle information
bd = bwboundaries(BW_inv);
cc = bwconncomp(BW_inv);
data = regionprops(cc,'basic');



% find clusters
c = 0;
for i = 1 : cc.NumObjects
    if data(i).Area >= 1492
        c = c +1;
    end
end
```

```
%%%%%% need to identify these clusters


% calculate distance among boundaries
Dist = zeros(PN, PN);
 for i = 1:PN
    for j = (i+1):PN
        [m,r] = size(bd{i,1});
        [n,r] = size(bd{j,1});
        for x = 1:m
            for y = 1:n
            dist_MN(x,y) =
sqrt((bd{i}(x,1)-bd{j}(y,1))^2+(bd{i}(x,2)-bd{j}(y,2))^2);
%           dist_MN(y,x) = dist_MN(x,y);
            end
        end
        Dist(i,j) = min(min(dist_MN));
        Dist(j,i) = Dist(i,j);
        clear dist_MN;
    end
 end

Max = max(max(Dist));



A = reshape(Dist,PN*PN,1);

B = sort(A);

F= find (B>7 & B<15);

i=0;
for i = 1: length(F)/2;
    D(i)=B (F(2*i));
end


%% sdfasdfadsfasf
[R,C]=find (Dist>0 & Dist<10.9);
sizeR=size(R);
for i=1:sizeR
bd1{i,1}=bd{R(i),1};
end
```

```
figure
imshow(BW_inv)
hold on
for i=1:sizeR
plot(bd1{i,1}(:,2),bd1{i,1}(:,1),'ro')
hold on
end

%%
[R1,C1]=find (Dist>16.35 & Dist<54.5);
sizeR1=size(R1);
for i=1:sizeR1
Dist_temp(i,1)=Dist(R1(i,1),C1(i,1));
end

for i = 1: sizeR1/2;
   Dist1(i,1)=Dist_temp(2*i);
end
```